Image Restoration

Image Restoration

- Image restoration: recover an image that has been degraded by using a prior knowledge of the degradation phenomenon.

- Model the degradation and applying the inverse process in order to recover the original image.

A Model of Image Degradation/Restoration Process

FIGURE 5.1
A model of the image degradation/ restoration process.

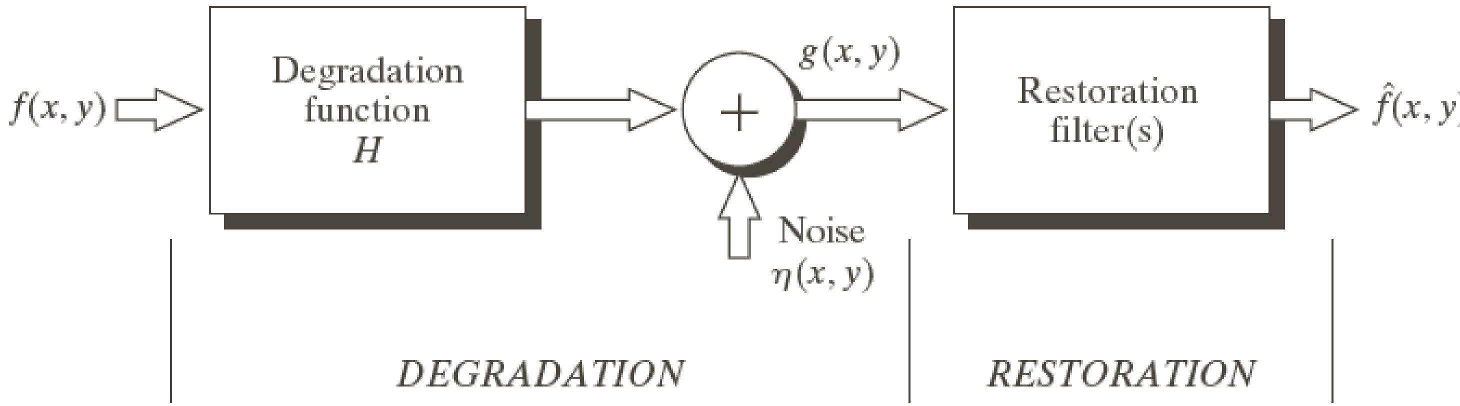

- Degradation
  - Degradation function H
  - Additive noise $\eta(x, y)$

A Model of Image Degradation/Restoration Process

FIGURE 5.1
A model of the image degradation/restoration process.

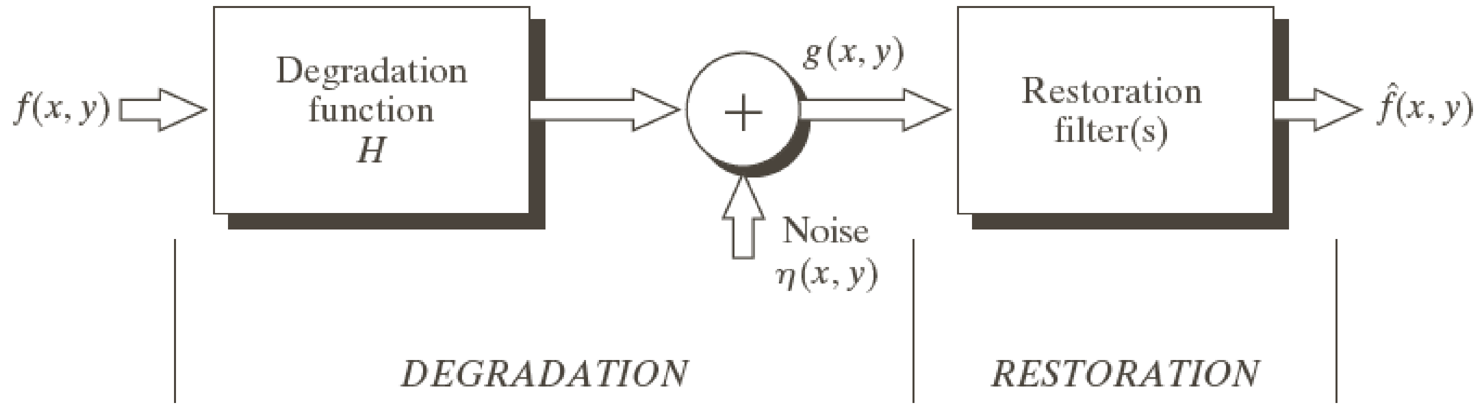

If H is a linear, position-invariant process, then the degraded image is given in the spatial domain by

$$g(x, y) = h(x, y) \star f(x, y) + \eta(x, y)$$

A Model of Image Degradation/Restoration Process

The model of the degraded image is given in the frequency domain by

$$G(u,v) = H(u,v)F(u,v) + N(u,v)$$

Noise Sources

- The principal sources of noise in digital images arise during **image acquisition and/or transmission**

- ✓ Image acquisition

  e.g., light levels, sensor temperature, etc.

- ✓ Transmission

  e.g., lightning or other atmospheric disturbance in wireless network

Noise Models (1)

- White noise
  - The Fourier spectrum of noise is constant

- With the exception of spatially periodic noise, we assume
  - Noise is independent of spatial coordinates
  - Noise is uncorrelated with respect to the image itself

Noise Models (2)

- **Gaussian noise**
  Electronic circuit noise, sensor noise due to poor illumination and/or high temperature
- **Rayleigh noise**
  Range imaging

Noise Models (3)

- **Erlang (gamma) noise**: Laser imaging
- **Exponential noise**: Laser imaging
- **Uniform noise**: Least descriptive; Basis for numerous random number generators
- **Impulse noise**: quick transients, such as faulty switching

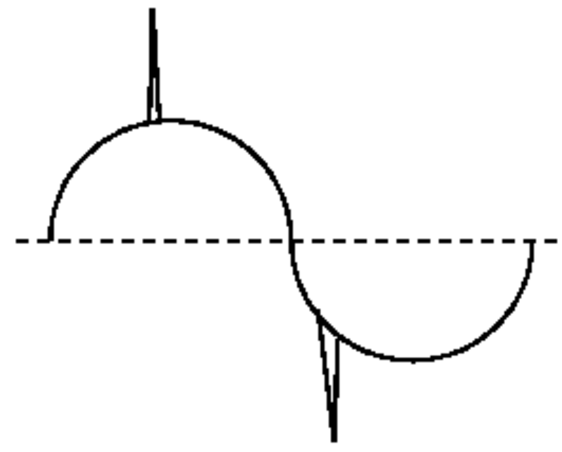

Impulse Noise

Gaussian Noise (1)

The PDF of Gaussian random variable, z, is given by

$$p(z) = \frac{1}{\sqrt{2\pi}\sigma} e^{-(z-\bar{z})^2/2\sigma^2}$$

where, z represents intensity

$\bar{z}$ is the mean (average) value of z

σ is the standard deviation

Gaussian Noise (2)

The PDF of Gaussian random variable, z, is given by

$$p(z) = \frac{1}{\sqrt{2\pi}\sigma} e^{-(z-\bar{z})^2/2\sigma^2}$$

- 70% of its values will be in the range

$$\left[(\mu-\sigma),(\mu+\sigma)\right]$$

- 95% of its values will be in the range

$$\left[(\mu-2\sigma),(\mu+2\sigma)\right]$$

Rayleigh Noise

The PDF of Rayleigh noise is given by

$$p(z) = \begin{cases} \frac{2}{b}(z-a)e^{-(z-a)^2/b} & \text{for } z \geq a \\ 0 & \text{for } z < a \end{cases}$$

The mean and variance of this density are given by

$$\bar{z} = a + \sqrt{\pi b / 4}$$

$$\sigma^2 = \frac{b(4-\pi)}{4}$$

Erlang (Gamma) Noise

The PDF of Erlang noise is given by

$$p(z) = \begin{cases} \dfrac{a^b z^{b-1}}{(b-1)!} e^{-az} & \text{for } z \geq 0 \\ 0 & \text{for } z < a \end{cases}$$

The mean and variance of this density are given by

$$\bar{z} = b / a$$

$$\sigma^2 = b / a^2$$

Exponential Noise

The PDF of exponential noise is given by

$$p(z) = \begin{cases} ae^{-az} & \text{for } z \geq 0 \\ 0 & \text{for } z < a \end{cases}$$

The mean and variance of this density are given by

$$\bar{z} = 1/a$$

$$\sigma^2 = 1/a^2$$

Uniform Noise

The PDF of uniform noise is given by

$$p(z) = \begin{cases} \dfrac{1}{b-a} & \text{for a} \le z \le b \\ 0 & \text{otherwise} \end{cases}$$

The mean and variance of this density are given by

$$\bar{z} = (a+b)/2$$

$$\sigma^2 = (b-a)^2/12$$

Impulse (Salt-and-Pepper) Noise

The PDF of (bipolar) impulse noise is given by

$$p(z) = \begin{cases} P_a & \text{for } z = a \\ P_b & \text{for } z = b \\ 0 & \text{otherwise} \end{cases}$$

if $b > a$, gray-level b will appear as a light dot, while level a will appear like a dark dot.

If either P_a or P_b is zero, the impulse noise is called *unipolar*

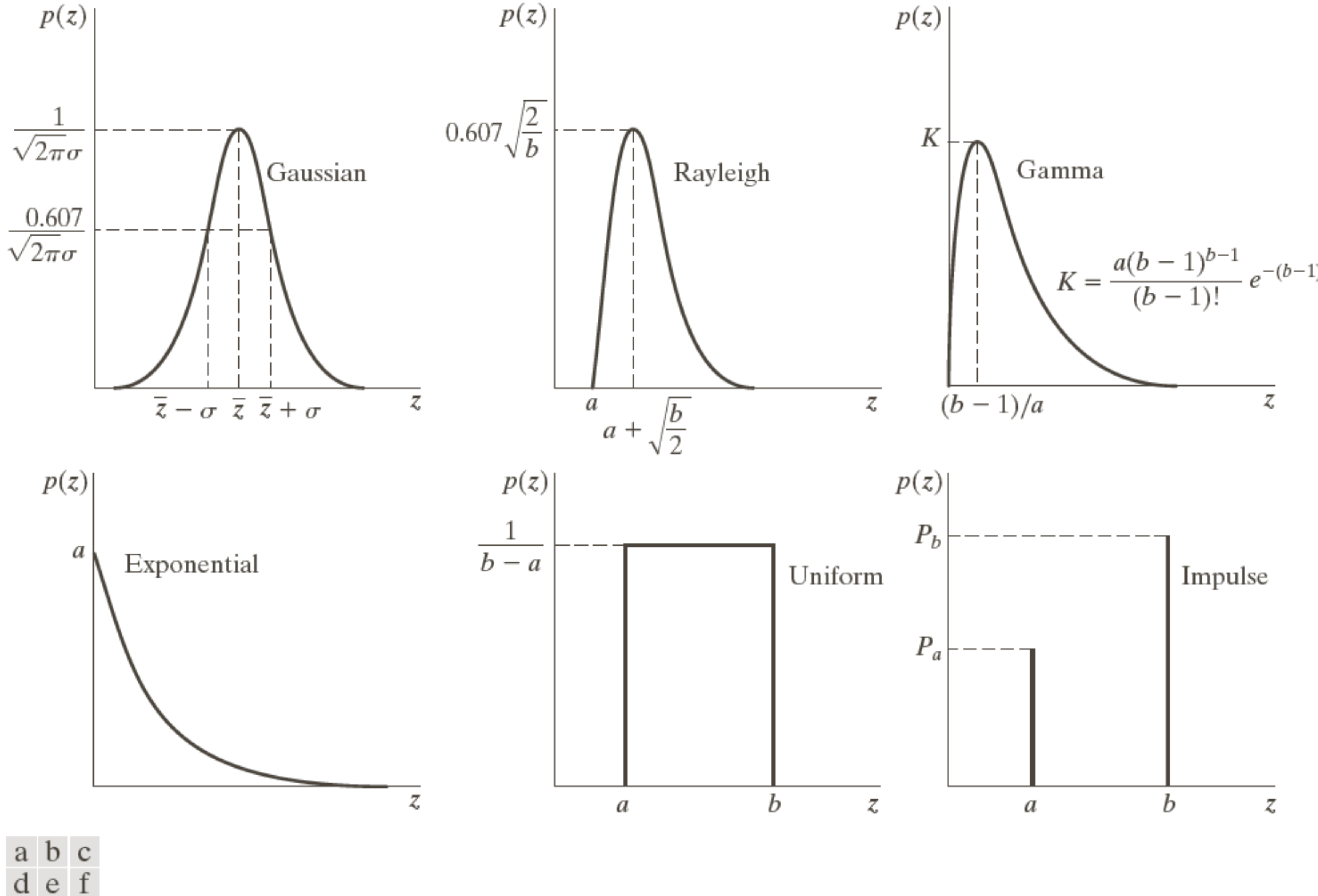

FIGURE 5.2 Some important probability density functions.

Examples of Noise: Original Image

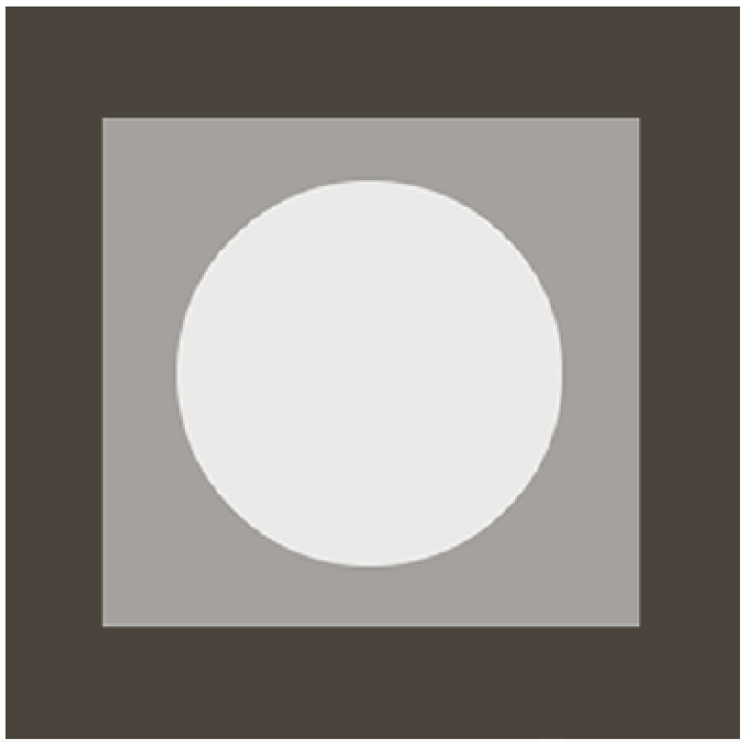

FIGURE 5.3 Test pattern used to illustrate the characteristics of the noise PDFs shown in Fig. 5.2.

Examples of Noise: Noisy Images(1)

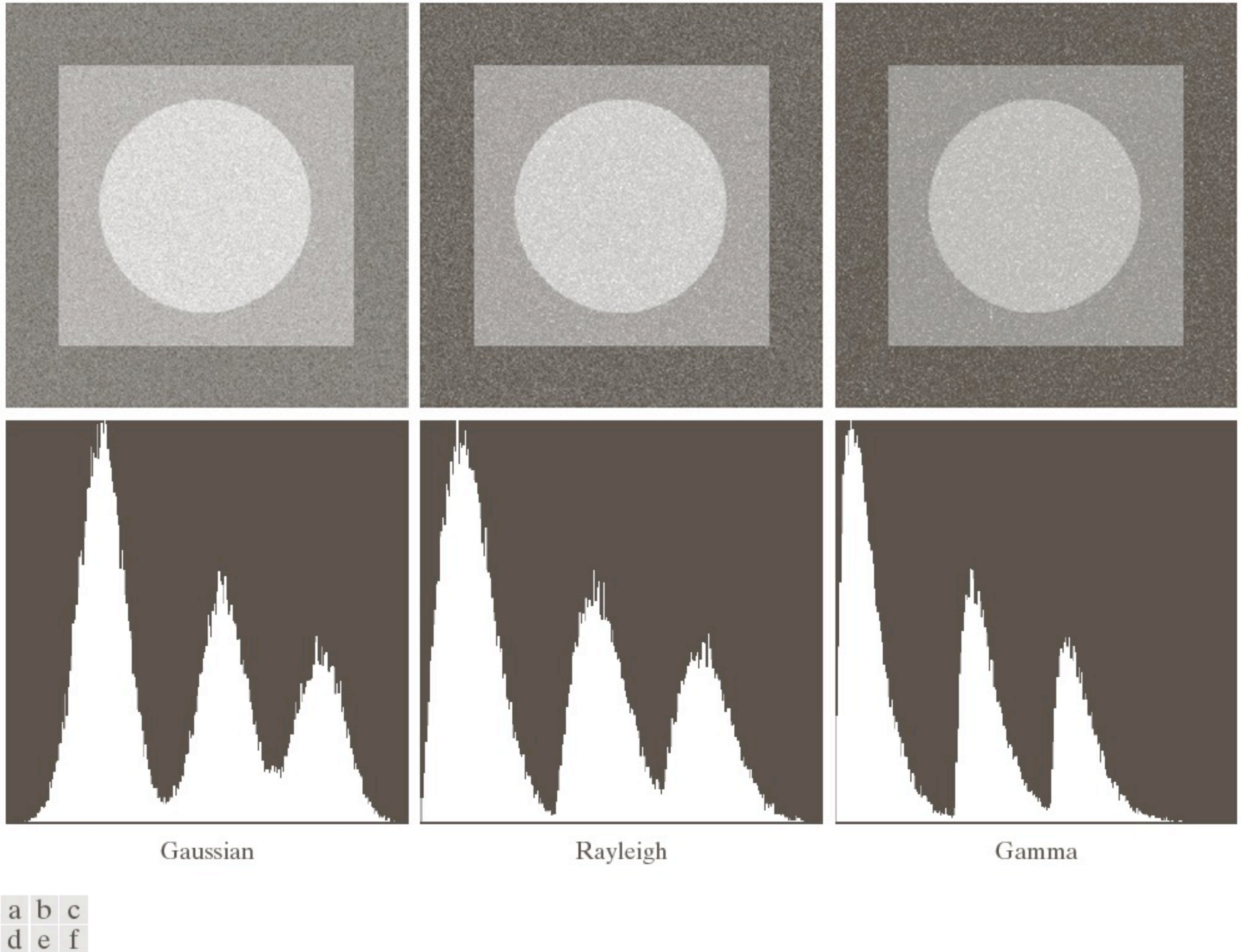

FIGURE 5.4 Images and histograms resulting from adding Gaussian, Rayleigh, and gamma noise to the image in Fig. 5.3.

Examples of Noise: Noisy Images(2)

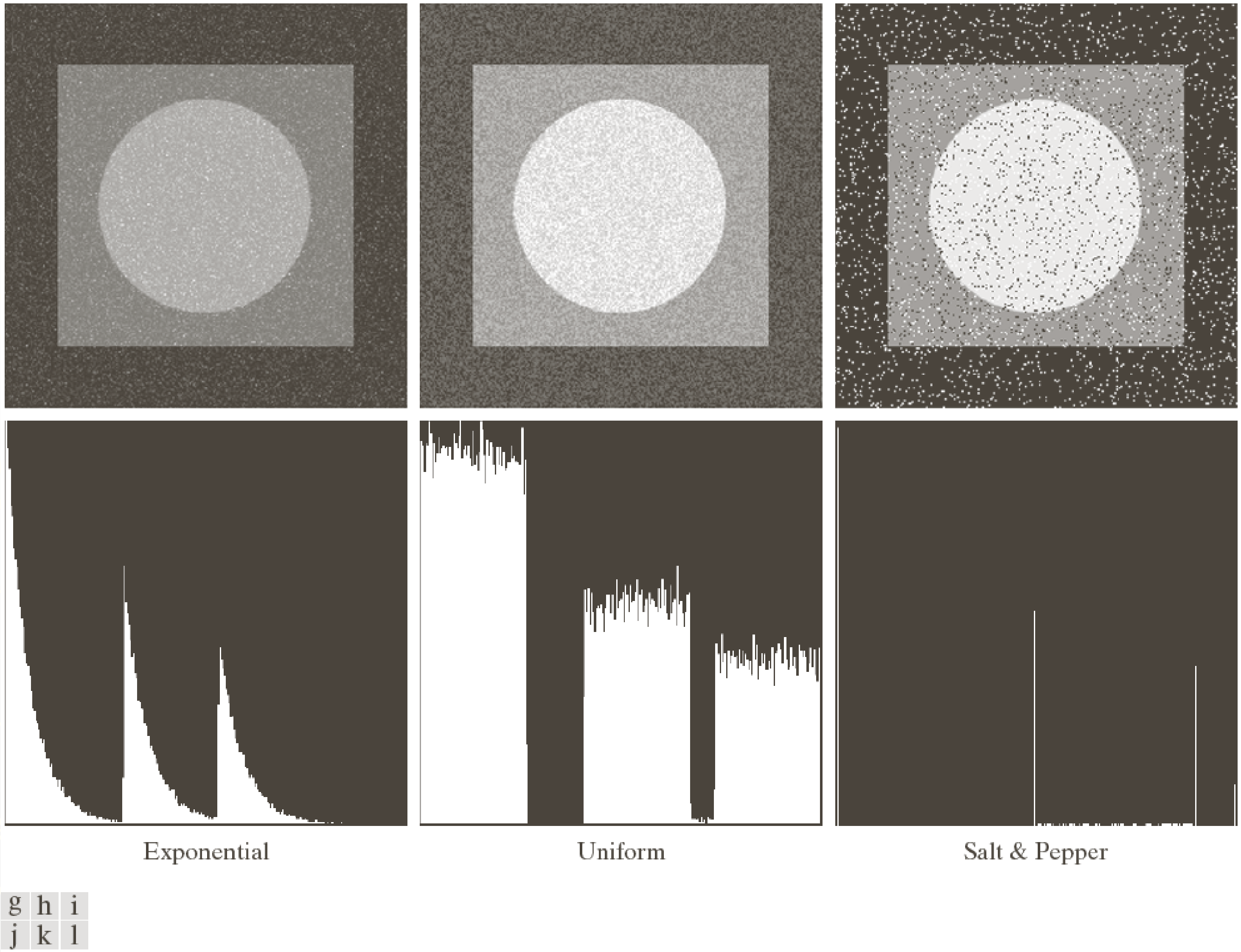

FIGURE 5.4 *(Continued)* Images and histograms resulting from adding exponential, uniform, and salt and pepper noise to the image in Fig. 5.3.

Periodic Noise

- Periodic noise in an image arises typically from electrical or electromechanical interference during image acquisition.
- It is a type of spatially dependent noise
- Periodic noise can be reduced significantly via frequency domain filtering

An Example of Periodic Noise

a
b

FIGURE 5.5
(a) Image corrupted by sinusoidal noise. (b) Spectrum (each pair of conjugate impulses corresponds to one sine wave). (Original image courtesy of NASA.)

Estimation of Noise Parameters (1)

The shape of the histogram identifies the closest PDF match

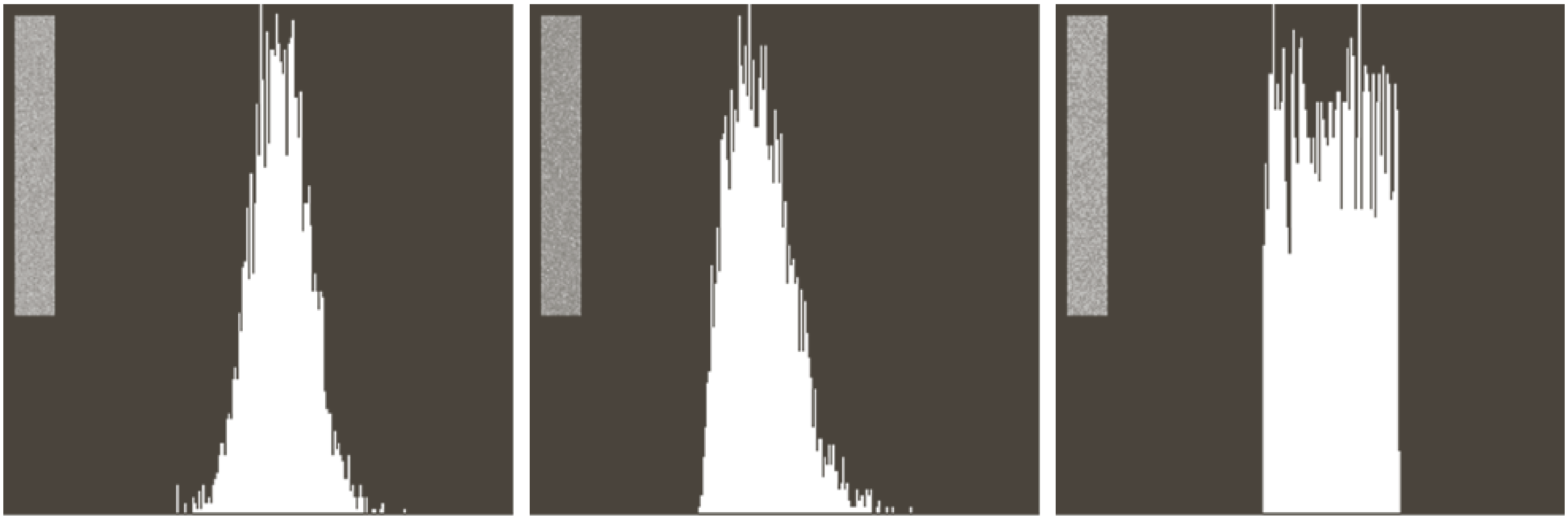

FIGURE 5.6 Histograms computed using small strips (shown as inserts) from (a) the Gaussian, (b) the Rayleigh, and (c) the uniform noisy images in Fig. 5.4.

Estimation of Noise Parameters (2)

Consider a subimage denoted by S, and let $p_s(z_i)$, $i = 0, 1, ..., L-1$, denote the probability estimates of the intensities of the pixels in S. The mean and variance of the pixels in S:

$$\bar{z} = \sum_{i=0}^{L-1} z_i p_s(z_i)$$

and

$$\sigma^2 = \sum_{i=0}^{L-1} (z_i - \bar{z})^2 p_s(z_i)$$

Restoration in the Presence of Noise Only – Spatial Filtering

Noise model without degradation

$$g(x, y) = f(x, y) + \eta(x, y)$$

and

$$G(u, v) = F(u, v) + N(u, v)$$

Spatial Filtering: Mean Filters (1)

Let S_{xy} represent the set of coordinates in a rectangle subimage window of size $m \times n$, centered at (x, y).

Arithmetic mean filter

$$\hat{f}(x, y) = \frac{1}{mn} \sum_{(s,t) \in S_{xy}} g(s, t)$$

Smooths local variation in an image;
Noise is reduced as a result of blurring

Spatial Filtering: Mean Filters (2)

Geometric mean filter

$$f(x,y) = \left[\prod_{(s,t)\in S_{xy}} g(s,t) \right]^{\frac{1}{mn}}$$

Generally, a geometric mean filter achieves smoothing comparable to the arithmetic mean filter, but it tends to lose less image detail in the process

Spatial Filtering: Mean Filters (3)

Harmonic mean filter

$$\hat{f}(x,y) = \frac{mn}{\displaystyle\sum_{(s,t)\in S_{xy}} \frac{1}{g(s,t)}}$$

It works well for salt noise, but fails for pepper noise.
It does well also with other types of noise like Gaussian noise.

Spatial Filtering: Mean Filters (4)

Contraharmonic mean filter

$$f(x,y) = \frac{\sum_{(s,t)\in S_{xy}} g(s,t)^{Q+1}}{\sum_{(s,t)\in S_{xy}} g(s,t)^{Q}}$$

Q is the order of the filter.

It is well suited for reducing the effects of salt-and-pepper noise. Q>0 for pepper noise and Q<0 for salt noise.

Spatial Filtering: Example (1)

a	b
c	d

FIGURE 5.7 (a) X-ray image. (b) Image corrupted by additive Gaussian noise. (c) Result of filtering with an arithmetic mean filter of size 3 × 3. (d) Result of filtering with a geometric mean filter of the same size. (Original image courtesy of Mr. Joseph E. Pascente, Lixi, Inc.)

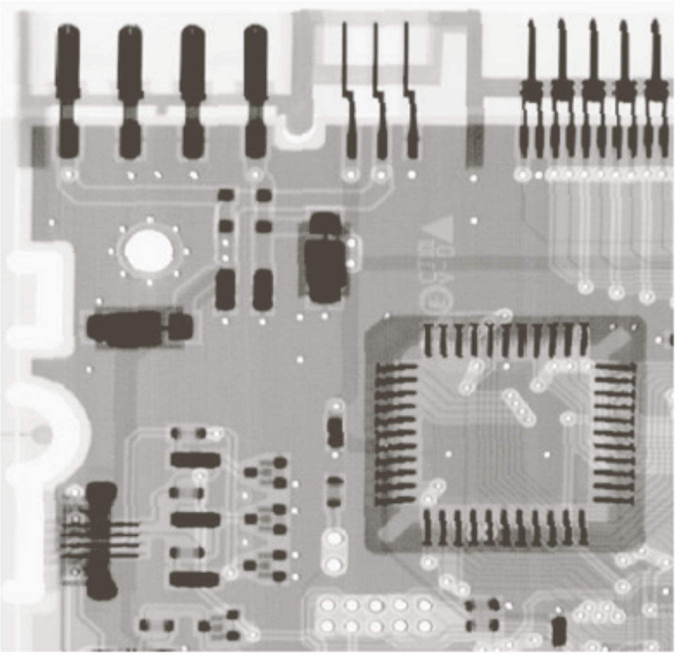

Spatial Filtering: Example (2)

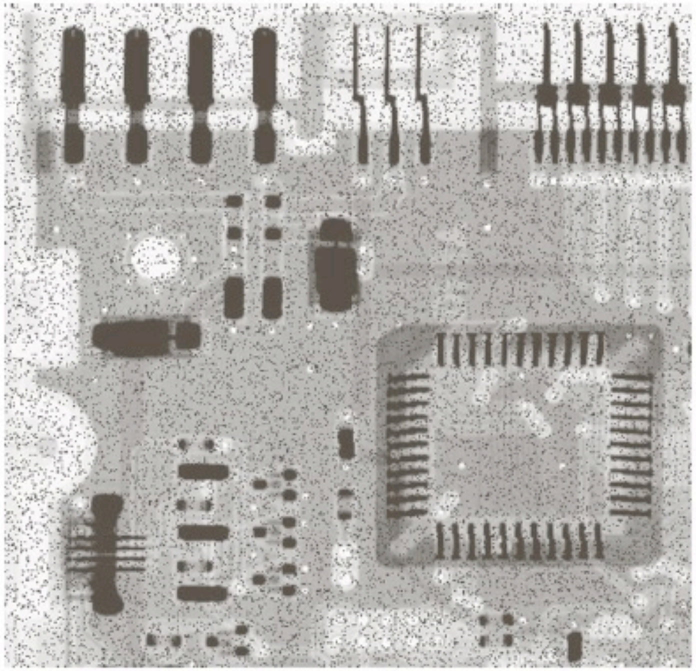

a b
c d

FIGURE 5.8
(a) Image corrupted by pepper noise with a probability of 0.1. (b) Image corrupted by salt noise with the same probability. (c) Result of filtering (a) with a 3×3 contra-harmonic filter of order 1.5. (d) Result of filtering (b) with $Q = -1.5$.

Spatial Filtering: Example (3)

a b

FIGURE 5.9 Results of selecting the wrong sign in contraharmonic filtering. (a) Result of filtering Fig. 5.8(a) with a contraharmonic filter of size 3×3 and $Q = -1.5$. (b) Result of filtering 5.8(b) with $Q = 1.5$.

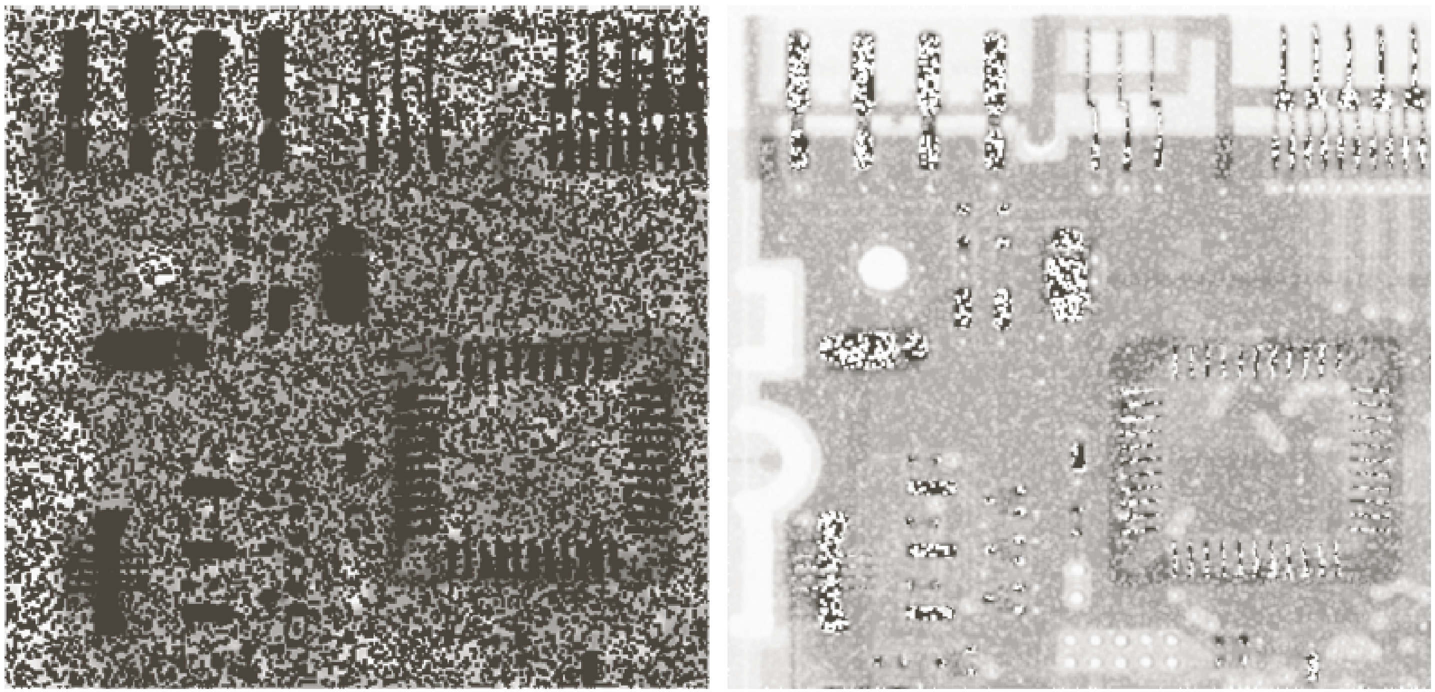

For contraharmonic filter, MUST know weather noise is Salt or pepper.

Spatial Filtering: Order-Statistic Filters (1)

Median filter

$$f(x,y) = \underset{(s,t)\in S_{xy}}{median}\{g(s,t)\}$$

Effective in the presence of both unipolar and bipolar noise

Max filter

$$f(x,y) = \max_{(s,t)\in S_{xy}}\{g(s,t)\}$$

Reduces pepper noise; finds brightest point in an image

Min filter

$$f(x,y) = \min_{(s,t)\in S_{xy}}\{g(s,t)\}$$

Reduces salt noise; finds darkest point in an image

Spatial Filtering: Order-Statistic Filters (2)

Midpoint filter

$$f(x,y)=\frac{1}{2}\left[\max_{(s,t)\in S_{xy}}\{g(s,t)\}+\min_{(s,t)\in S_{xy}}\{g(s,t)\}\right]$$

Combines order statistics and averaging
Works best for randomly distributed noise e.g. Gaussian or unfiorm

Spatial Filtering: Order-Statistic Filters (3)

Alpha-trimmed mean filter

$$f(x,y) = \frac{1}{mn-d} \sum_{(s,t)\in S_{xy}} \{g_r(s,t)\}$$

We delete the $d/2$ lowest and the $d/2$ highest intensity values of $g(s,t)$ in the neighborhood S_{xy}. Let $g_r(s,t)$ represent the remaining $mn - d$ pixels.

- Useful with multiple types of noise, e.g. combination of salt and pepper and Gaussian noise.
- if d = mn -1 , reduces to median filter

a	b
c	d

FIGURE 5.10
(a) Image corrupted by salt-and-pepper noise with probabilities $P_a = P_b = 0.1$.
(b) Result of one pass with a median filter of size 3×3.
(c) Result of processing (b) with this filter.
(d) Result of processing (c) with the same filter.

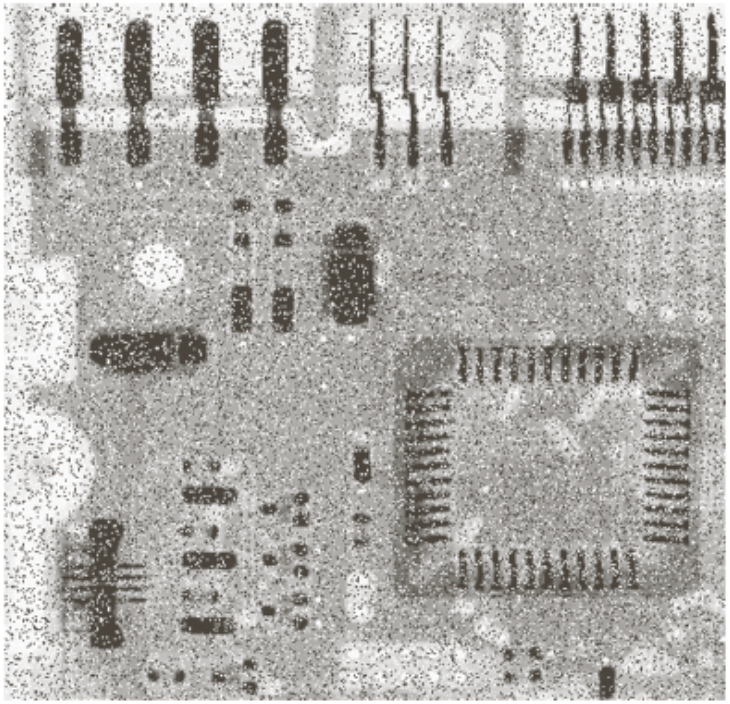

Repeated median filtering blurs

a b

FIGURE 5.11
(a) Result of filtering Fig. 5.8(a) with a max filter of size 3 × 3. (b) Result of filtering 5.8(b) with a min filter of the same size.

Max filter removes some dark pixels
Min filter removes some light pixels

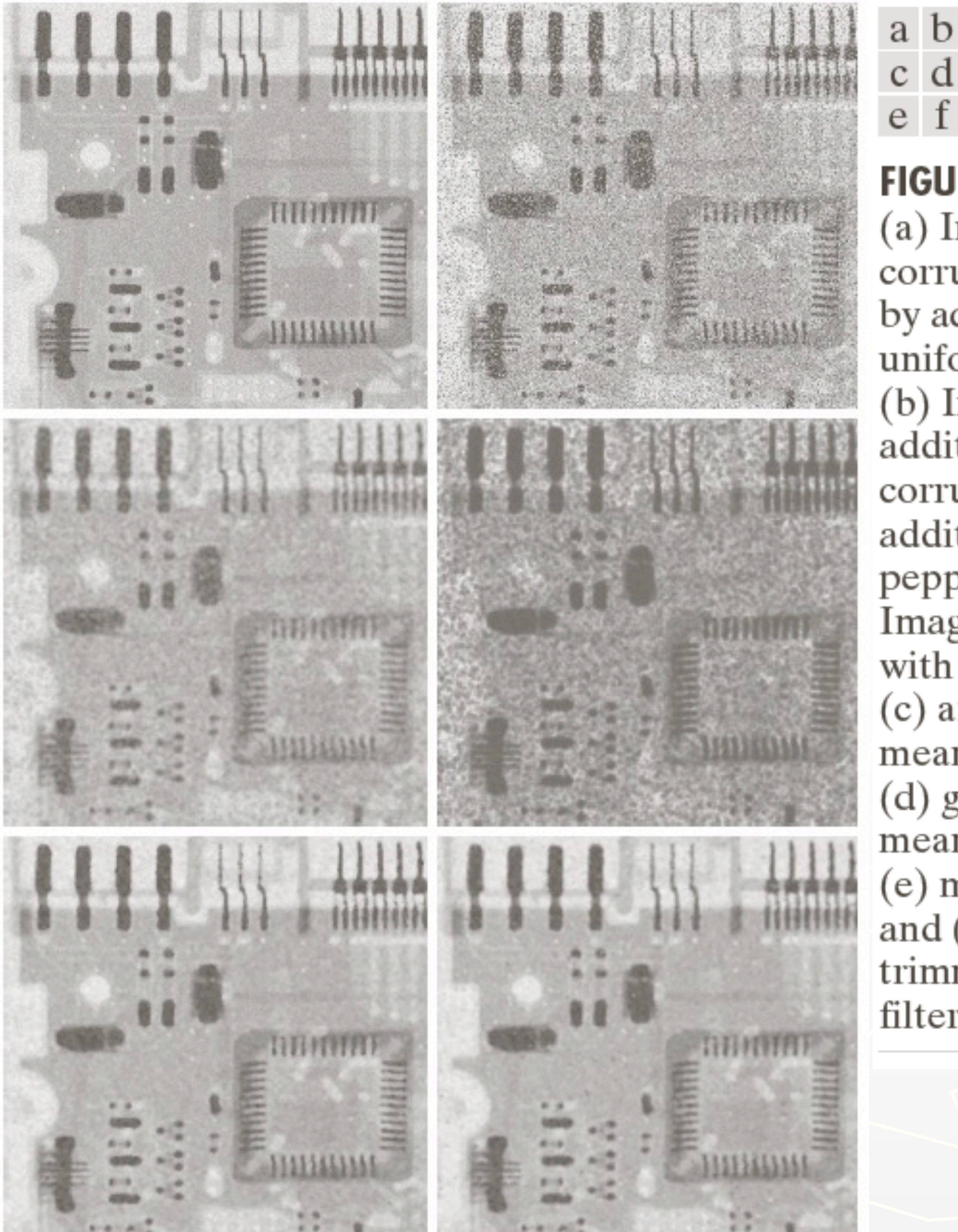

FIGURE 5.12 (a) Image corrupted by additive uniform noise. (b) Image additionally corrupted by additive salt-and-pepper noise. Image (b) filtered with a 5×5; (c) arithmetic mean filter; (d) geometric mean filter; (e) median filter; and (f) alpha-trimmed mean filter with $d = 5$.

Spatial Filtering: Adaptive Filters (1)

Adaptive filters

The behavior changes based on statistical characteristics of the image inside the filter region defined by the mxn rectangular window.

The performance is superior to that of the filters discussed

Adaptive Filters:
Adaptive, Local Noise Reduction Filters (1)

S_{xy}: local region

The response of the filter at the center point (x,y) of S_{xy} is based on four quantities:

(a) $g(x, y)$, the value of the noisy image at (x, y);

(b) σ_η^2, the variance of the noise corrupting $f(x, y)$ to form $g(x, y)$;

(c) m_L, the local mean of the pixels in S_{xy};

(d) σ_L^2, the local variance of the pixels in S_{xy}.

Adaptive Filters: Adaptive, Local Noise Reduction Filters (2)

The behavior of the filter:

(a) if σ_η^2 is zero, the filter should return simply the value of $g(x, y)$.

(b) if the local variance is high relative to σ_η^2, the filter should return a value close to $g(x, y)$;

(c) if the two variances are equal, the filter returns the arithmetic mean value of the pixels in S_{xy}.

Adaptive Filters:
Adaptive, Local Noise Reduction Filters (3)

An adaptive expression for obtaining $f(x, y)$ based on the assumptions:

$$f(x, y) = g(x, y) - \frac{\sigma_\eta^2}{\sigma_L^2}\left[g(x, y) - m_L\right]$$

a	b
c	d

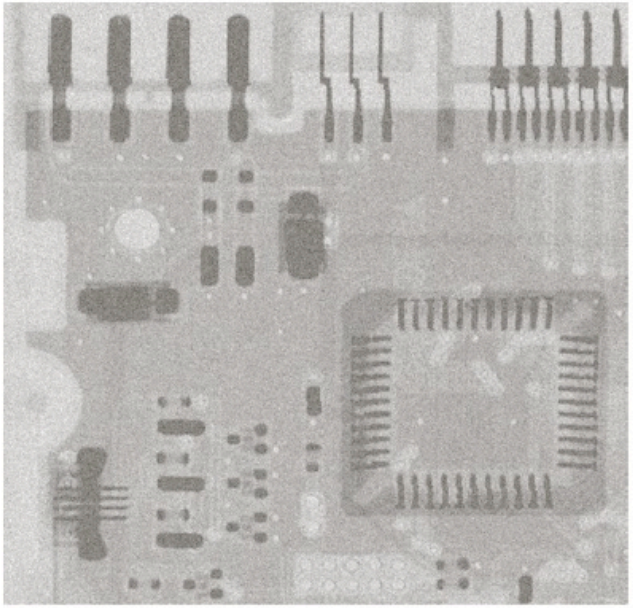

FIGURE 5.13
(a) Image corrupted by additive Gaussian noise of zero mean and variance 1000. (b) Result of arithmetic mean filtering. (c) Result of geometric mean filtering. (d) Result of adaptive noise reduction filtering. All filters were of size 7×7.

Shortcomings of Median Filtering

- Works only if spatial density of impulse noise is not large (Pa and Pb smaller than 0.2)
- Adaptive median filter works for large Pa and Pb
  - Preserves details while smoothing non-impulse noise
  - Median filter cannot do this.

Adaptive Filters:
Adaptive Median Filters (1)

The notation:

z_{min} = minimum intensity value in S_{xy}

z_{max} = maximum intensity value in S_{xy}

z_{med} = median intensity value in S_{xy}

z_{xy} = intensity value at coordinates (x, y)

S_{max} = maximum allowed size of S_{xy}

Intuition behind adaptive median filter

- Keep increasing window size until z_med is not an impulse, i.e.

  z_min < z_med < z_max

- When this happens check z_xy
  - If z_xy is not an impulse output z_xy
  - If z_xy is an impulse output z_med

  (since z_med is guaranteed not to be an impulse)

Adaptive Filters:
Adaptive Median Filters (2)

The adaptive median-filtering works in two stages:

Stage A:

$A1 = z_{\mathrm{med}} - z_{\min}$; $A2 = z_{\mathrm{med}} - z_{\max}$

if A1>0 and A2<0, go to stage B

Else increase the window size

if window size $\leq S_{\max}$, repeat stage A; Else output z_{med}

Stage B:

$B1 = z_{xy} - z_{\min}$; $B2 = z_{xy} - z_{\max}$

if B1>0 and B2<0, output z_{xy}; Else output z_{med}

Adaptive Filters:
Adaptive Median Filters (2)

The adaptive median-filtering works in two stages:

Stage A:

$A1 = z_{med} - z_{min}$; $A2 = z_{med} - z$

if A1>0 and A2<0, go to stage B

Else increase the window size

if window size $\leq S_{max}$, repeat stage A; Else output z_{med}

The median filter output is an impulse or not

Stage B:

$B1 = z_{xy} - z_{min}$; $B2 = z_{xy} - z$

if B1>0 and B2<0, output z_{xy}; Else output z_{med}

The processed point is an impulse or not

Example:
Adaptive Median Filters

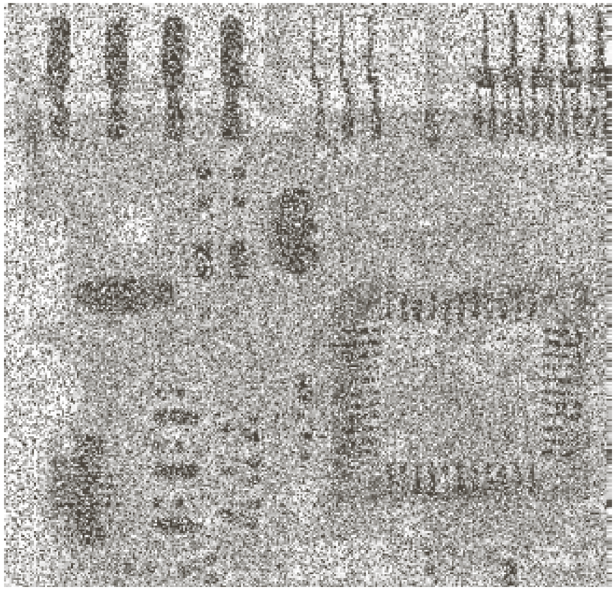

a b c

FIGURE 5.14 (a) Image corrupted by salt-and-pepper noise with probabilities $P_a = P_b = 0.25$. (b) Result of filtering with a 7×7 median filter. (c) Result of adaptive median filtering with $S_{max} = 7$.

Periodic Noise Reduction by Frequency Domain Filtering

The basic idea

Periodic noise appears as concentrated bursts of energy in the Fourier transform, at locations corresponding to the frequencies of the periodic interference

Approach

A selective filter is used to isolate the noise

Perspective Plots of Bandreject Filters

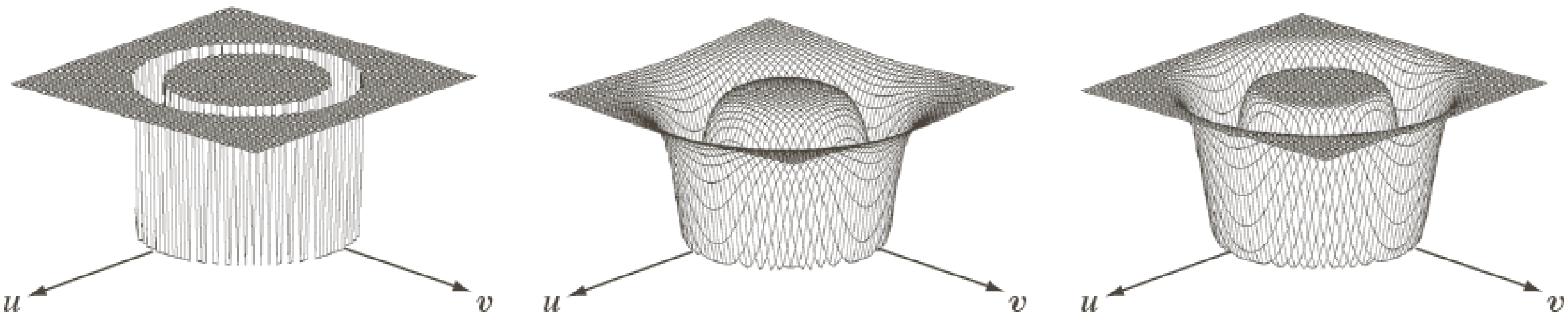

a b c

FIGURE 5.15 From left to right, perspective plots of ideal, Butterworth (of order 1), and Gaussian bandreject filters.

a b
c d

FIGURE 5.16
(a) Image corrupted by sinusoidal noise. (b) Spectrum of (a). (c) Butterworth bandreject filter (white represents 1). (d) Result of filtering. (Original image courtesy of NASA.)

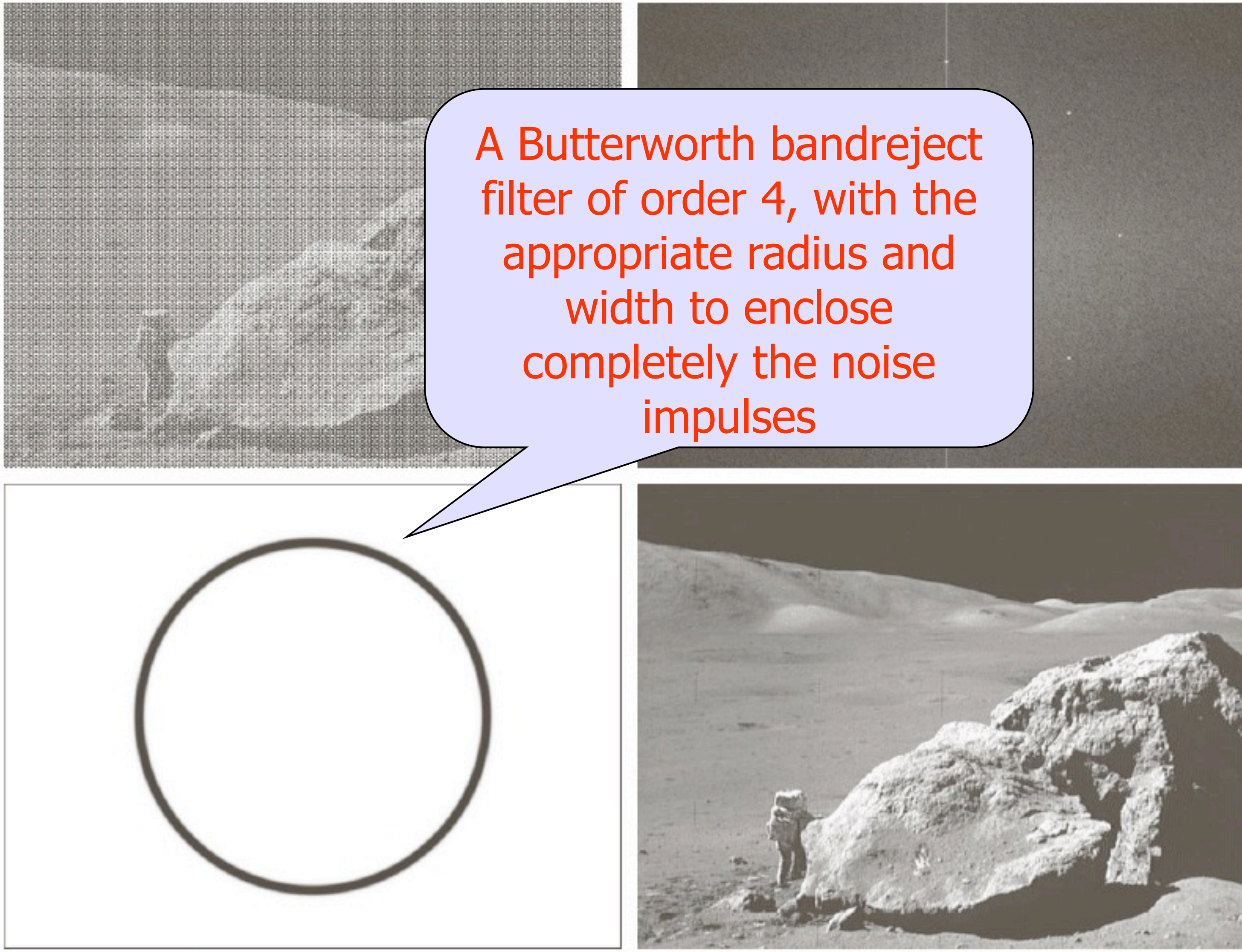

A Butterworth bandreject filter of order 4, with the appropriate radius and width to enclose completely the noise impulses

Perspective Plots of Notch Filters

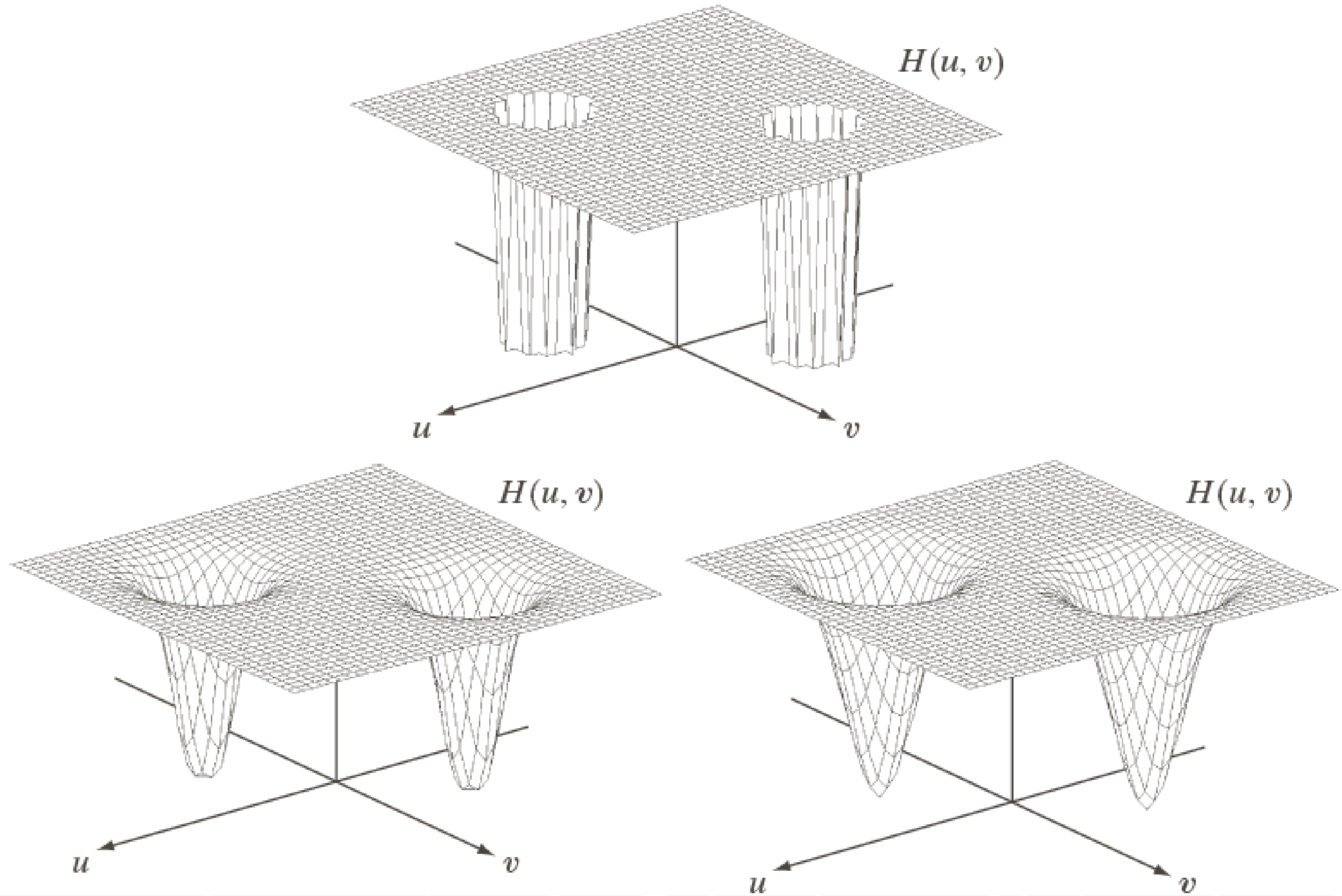

FIGURE 5.18 Perspective plots of (a) ideal, (b) Butterworth (of order 2), and (c) Gaussian notch (reject) filters.

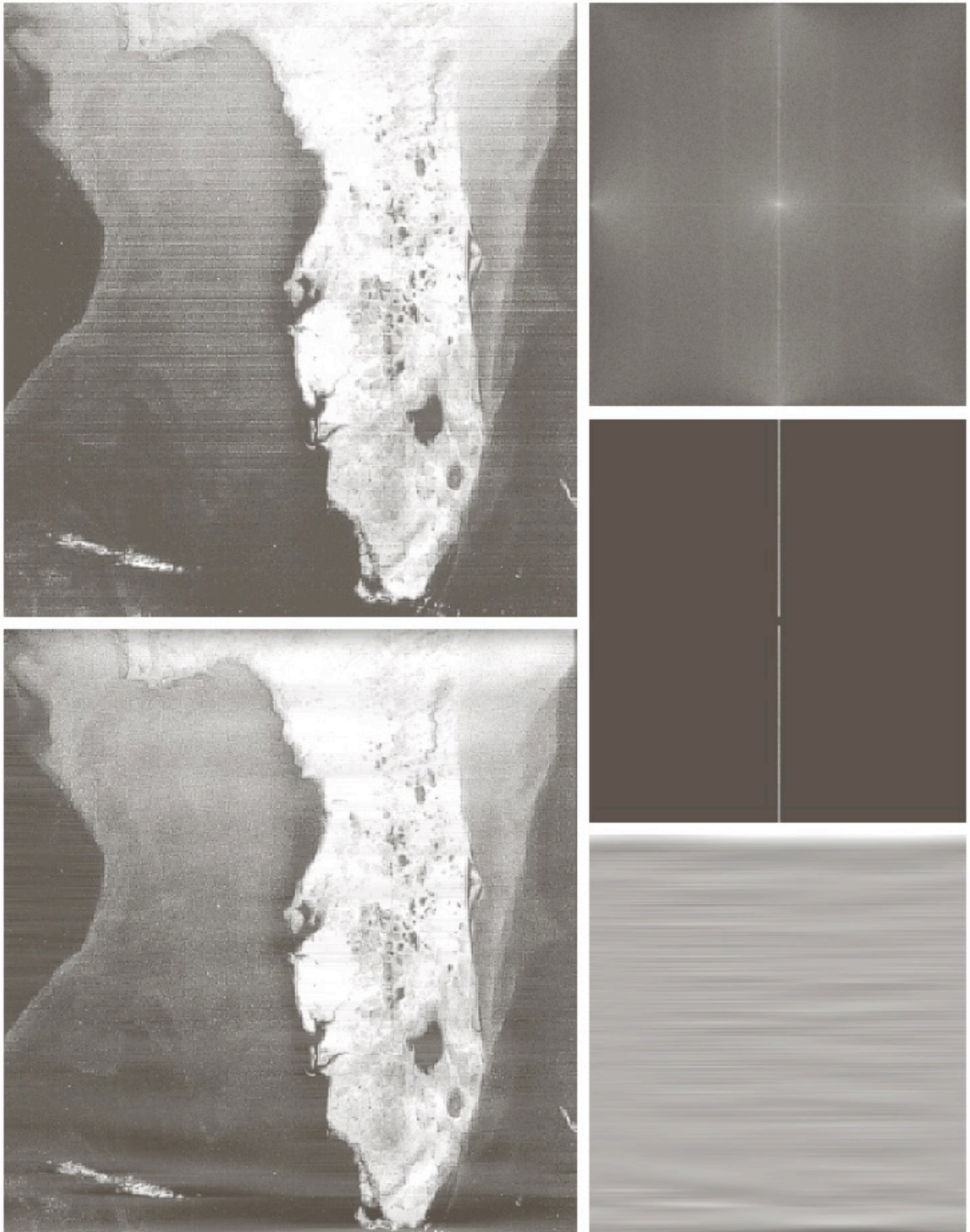

a b c d e

FIGURE 5.19 (a) Satellite image of Florida and the Gulf of Mexico showing horizontal scan lines. (b) Spectrum. (c) Notch pass filter superimposed on (b). (d) Spatial noise pattern. (e) Result of notch reject filtering. (Original image courtesy of NOAA.)

a b

FIGURE 5.20 (a) Image of the Martian terrain taken by *Mariner 6*. (b) Fourier spectrum showing periodic interference. (Courtesy of NASA.)

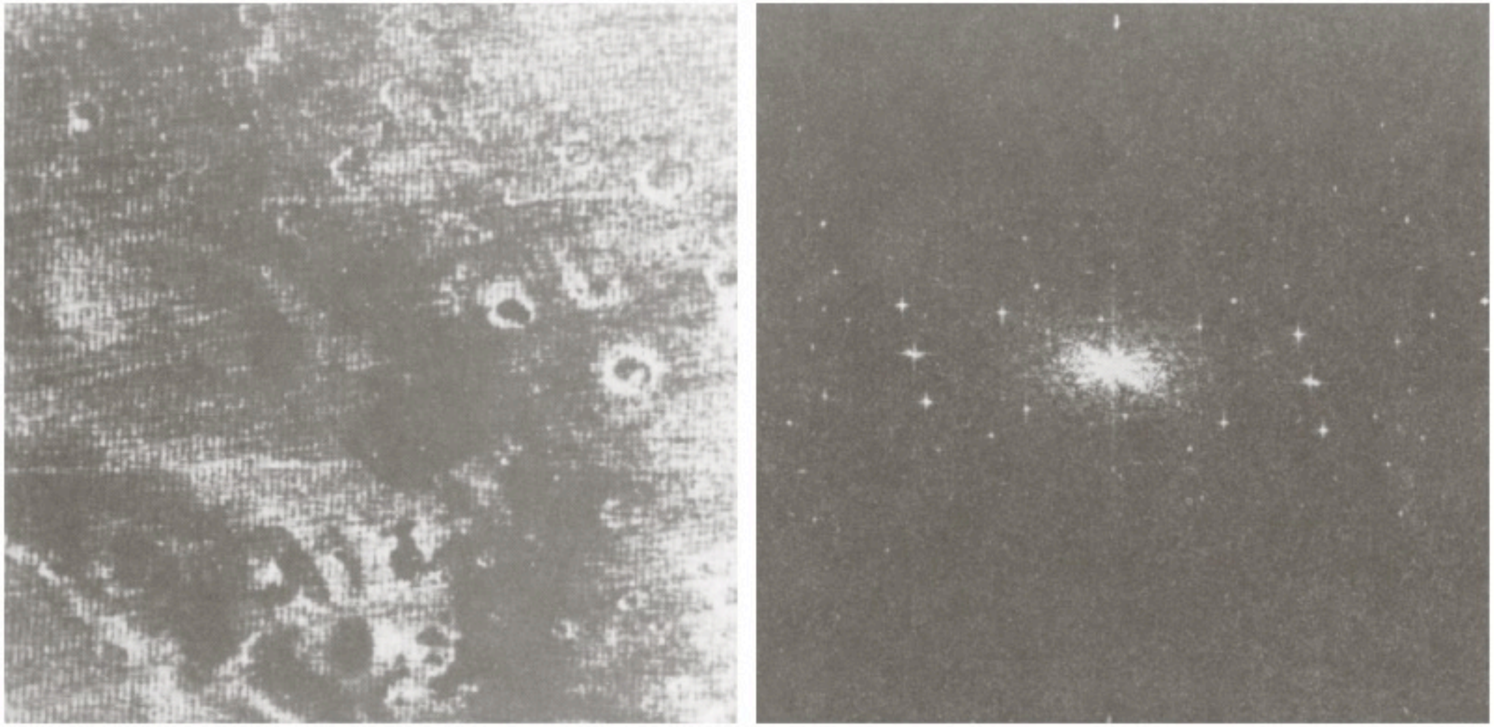

Several interference components are present, the methods discussed in the preceding sections are not always acceptable because they remove much image information

The components tend to have broad skirts that carry information about the interference pattern and the skirts are not always easily detectable.

Optimum Notch Filtering

It minimizes local variances of the restored estimated

$f(x, y)$

Procedure for restoration tasks in multiple periodic interference

Isolate the principal contributions of the interference pattern

Subtract a variable, weighted portion of the pattern from the corrupted image

Optimum Notch Filtering: Step 1

Extract the principal frequency components of the interference pattern

Place a notch pass filter at the location of each spike.

$$N(u,v) = H_{NP}(u,v)G(u,v)$$

$$\eta(x,y) = \Im^{-1}\left\{H_{NP}(u,v)G(u,v)\right\}$$

Optimum Notch Filtering: Step 2 (1)

Filtering procedure usually yields only an approximation of the true pattern. The effect of components not present in the estimate of $\eta(x, y)$ can be minimized instead by subtracting from $g(x, y)$ a weighted portion of $\eta(x, y)$ to obtain an estimate of $f(x, y)$:

$$f(x, y) = g(x, y) - w(x, y)\eta(x, y)$$

One approach is to select $w(x, y)$ so that the variance of the estimate $f(x, y)$ is minimized over a specified neighborhood of every point (x, y).

Optimum Notch Filtering: Step 2 (2)

The local variance of $f(x, y)$:

$$\sigma^2(x,y) = \frac{1}{(2a+1)(2b+1)} \sum_{s=-a}^{a} \sum_{t=-b}^{b} \left[f(x+s, y+t) - \overline{f}(x,y) \right]^2$$

Assume that w(x,y) remains essentially constant over the neighborhood gives the approximation
w(x+s, y+t) = w(x,y)

...ch Filtering: Step (3)

...):

$$\sigma^2(x,y) = \frac{1}{(2a+1)(2b+1)} \sum_{s=-a}^{a} \sum_{t=-b}^{b} \left[f(x+s, y+t) - \bar{f}(x,y) \right]^2$$

Optimum Notch Filtering: Step (4)

The local variance of $f(x, y)$:

$$\sigma^2(x,y) = \frac{1}{(2a+1)(2b+1)} \sum_{s=-a}^{a} \sum_{t=-b}^{b} \left\{ \begin{array}{l} \left[g(x+s, y+t) - w(x,y)\eta(x+s, y+s) \right] \\ - \left[\overline{g}(x,y) - w(x,y)\overline{\eta(x,y)} \right] \end{array} \right\}^2$$

Optimum Notch Filtering: Example

a b

FIGURE 5.20
(a) Image of the Martian terrain taken by *Mariner 6*. (b) Fourier spectrum showing periodic interference. (Courtesy of NASA.)

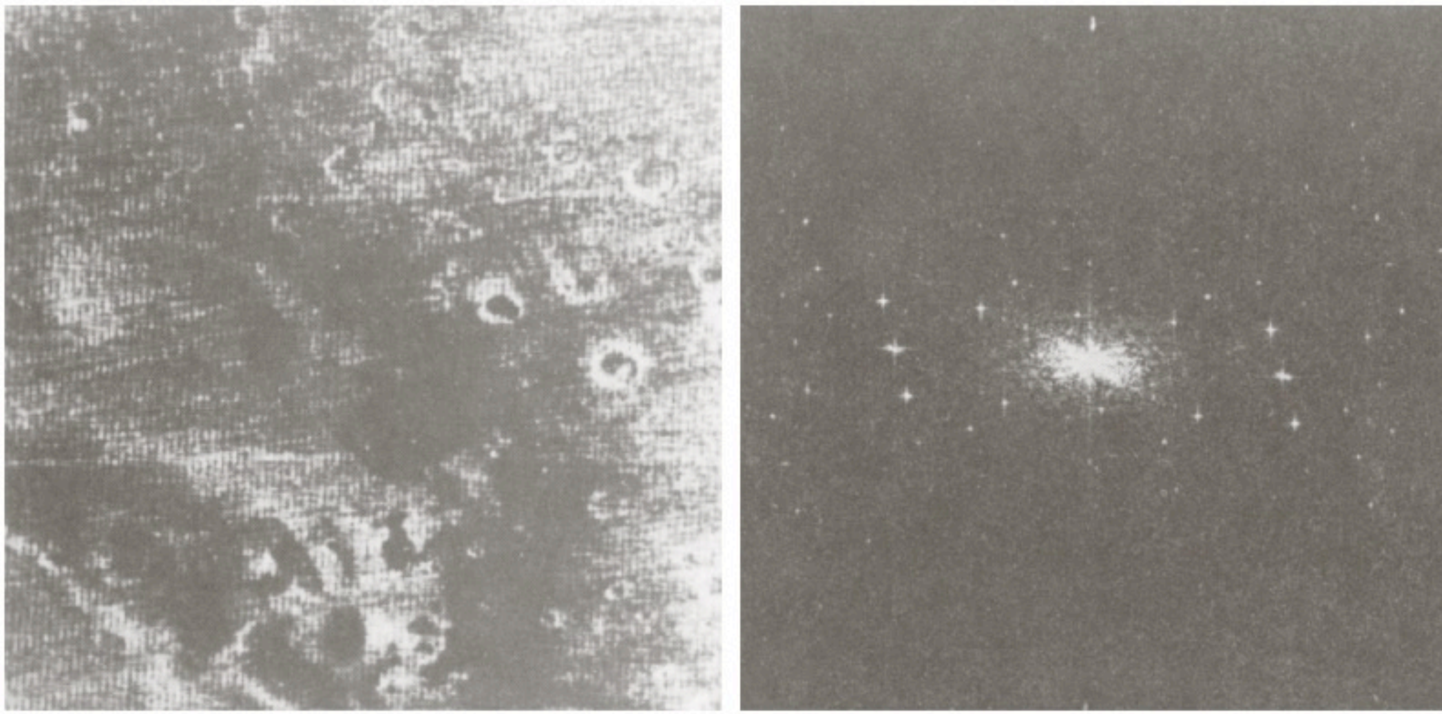

Optimum Notch Filtering: Example

FIGURE 5.21
Fourier spectrum (without shifting) of the image shown in Fig. 5.20(a). (Courtesy of NASA.)

Optimum Notch Filtering: Example

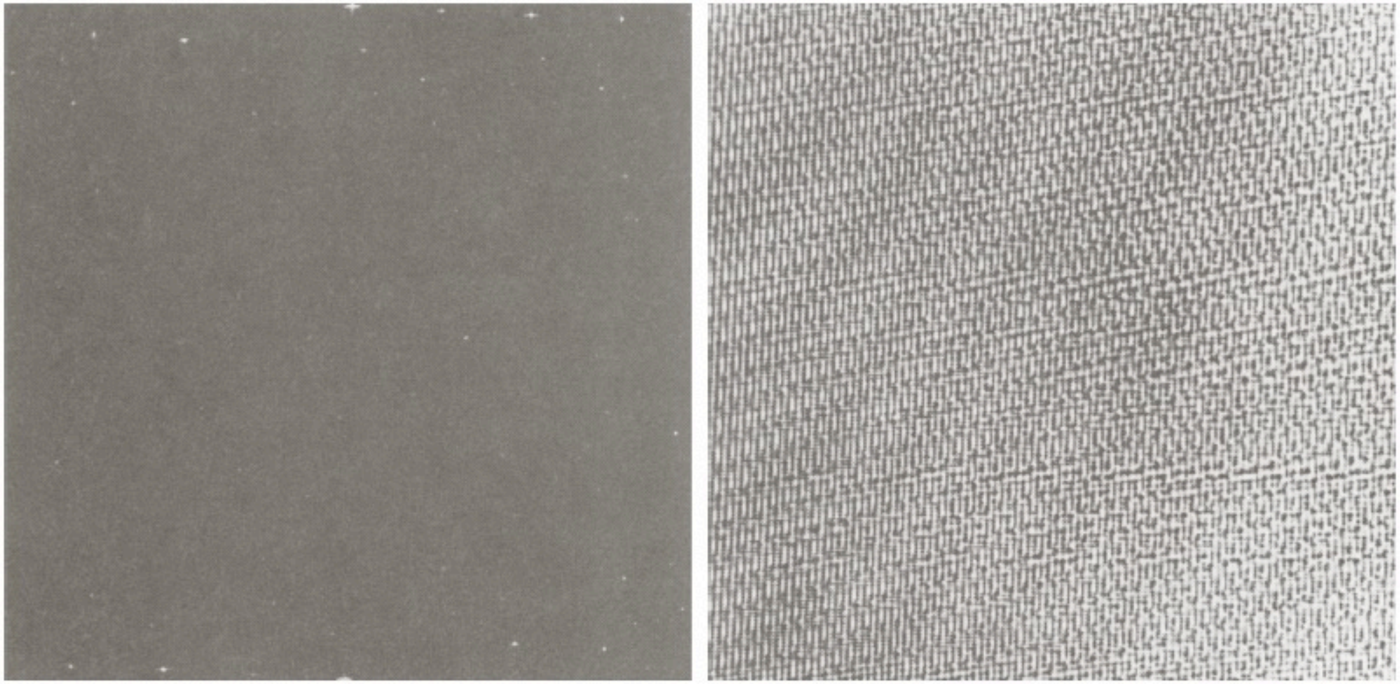

a b

FIGURE 5.22 (a) Fourier spectrum of $N(u, v)$, and (b) corresponding noise interference pattern $\eta(x, y)$. (Courtesy of NASA.)

Optimum Notch Filtering: Example

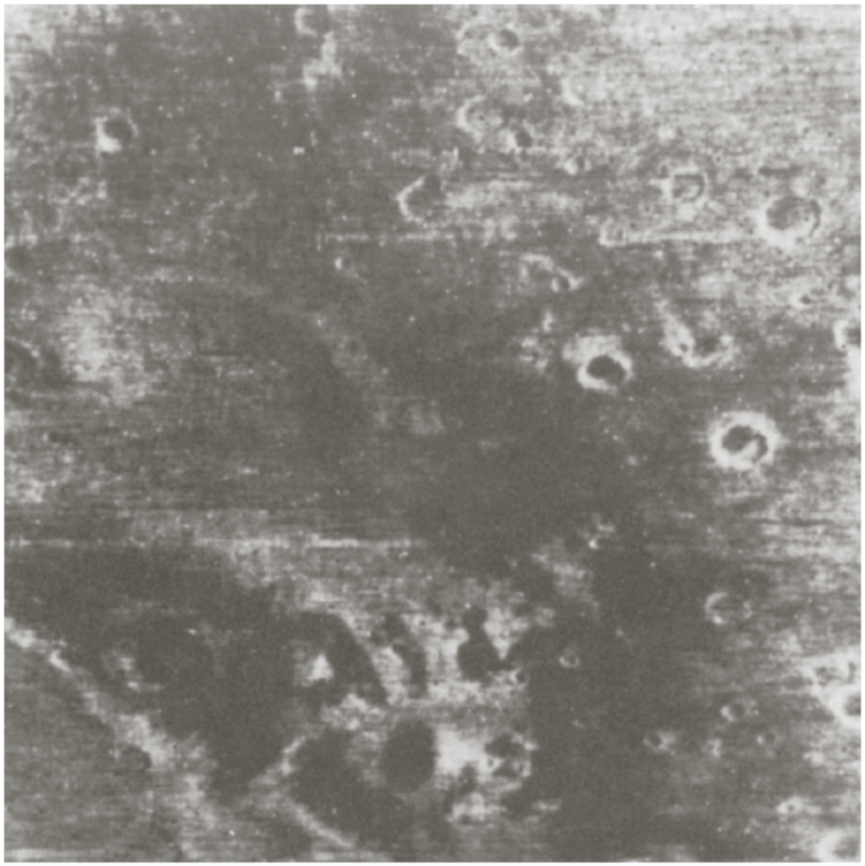

FIGURE 5.23
Processed image. (Courtesy of NASA.)

Linear, Position-Invariant Degradations

FIGURE 5.1 A model of the image degradation/restoration process.

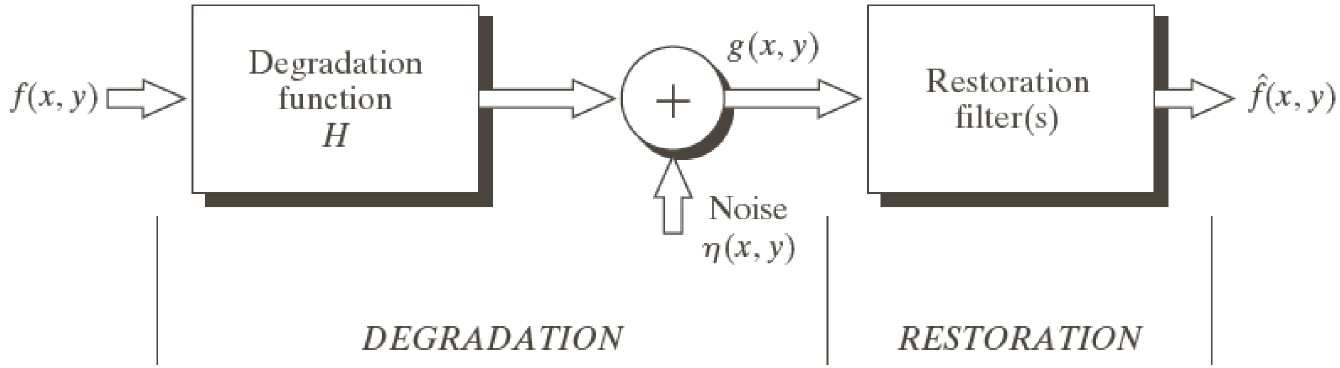

$$g(x,y) = H\left[f(x,y)\right] + \eta(x,y)$$

Linear, Position-Invariant Degradations

H is linear

$$H\left[af_1(x,y)+bf_2(x,y)\right]=aH\left[f_1(x,y)\right]+bH\left[f_2(x,y)\right]$$

f_1 and f_2 are any two input images.

An operator having the input-output relationship

$g(x,y)=H\left[f(x,y)\right]$ is said to be position invariant

if

$$H\left[f(x-\alpha,y-\beta)\right]=g(x-\alpha,y-\beta)$$

for any $f(x,y)$ and any α and β.

Linear, Position-Invariant Degradations

$$f(x,y)=\int_{-\infty}^{\infty}\int_{-\infty}^{\infty} f(\alpha,\beta)\delta(x-\alpha,y-\beta)\,d\alpha\, d\beta$$

Assume for a moment that $\eta(x,y)=0$

if H is a linear operator,

tion (or
lm)
of the
ind

se
se

Linear, Position-Invariant Degradations

Assume for a moment that $\eta(x, y) = 0$

if H is a linear operator and position invariant,

$$H\left[\delta(x-\alpha, y-\beta)\right] = h(x-\alpha, y-\beta)$$

$$g(x, y) = H\left[f(x, y)\right]$$

$$= \int_{-\infty}^{\infty}\int_{-\infty}^{\infty} f(\alpha, \beta) H\left[\delta(x-\alpha, y-\beta)\right] d\alpha\, d\beta$$

Convolution integral in 2-D

Linear, Position-Invariant Degradations

In the presence of additive noise,

if H is a linear operator and position invariant,

$$g(x,y) = \int_{-\infty}^{\infty}\int_{-\infty}^{\infty} f(\alpha,\beta)h(x-\alpha,y-\beta)\,d\alpha\,d\beta + \eta(x,y)$$

$$= h(x,y) \star f(x,y) + \eta(x,y)$$

$$G(u,v) = H(u,v)F(u,v) + N(u,v)$$

Estimating the Degradation Function

- Three principal ways to estimate the degradation function

1. Observation

2. Experimentation

3. Mathematical Modeling

Mathematical Modeling (1)

- Environmental conditions cause degradation

A model about atmospheric turbulence

$$H(u,v) = e^{-k(u^2+v^2)^{5/6}}$$

k : a constant that depends on the nature of the turbulence

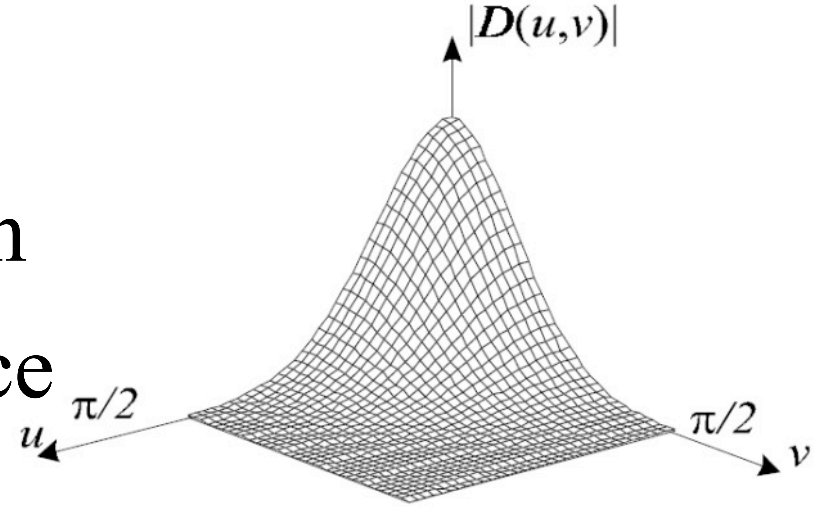

Gaussian PSF in the Fourier domain (σ_G=1.2).

a	b
c	d

FIGURE 5.25 Illustration of the atmospheric turbulence model. (a) Negligible turbulence. (b) Severe turbulence, $k = 0.0025$. (c) Mild turbulence, $k = 0.001$. (d) Low turbulence, $k = 0.00025$. (Original image courtesy of NASA.)

Mathematical Modeling (2)

- Derive a mathematical model from basic principles

E.g., An image blurred by uniform linear motion between the image and the sensor during image acquisition

Mathematical Modeling (3)

Suppose that an image $f(x, y)$ undergoes planar motion, $x_0(t)$ and $y_0(t)$ are the time-varying components of motion in the x- and y-directions, respectively.

The optical imaging process is perfect. T is the duration of the exposure. The blurred image $g(x, y)$

$$g(x, y) = \int_0^T f\left[x - x_0(t), y - y_0(t)\right] dt$$

Mathematical Modeling (4)

$$g(x, y) = \int_0^T f\left[x - x_0(t), y - y_0(t)\right] dt$$

$$G(u, v) = \int_{-\infty}^{\infty} \int_{-\infty}^{\infty} g(x, y) e^{-j2\pi(ux+vy)} dxdy$$

Mathematical Modeling (4)

$$H(u,v)=\int_0^T e^{-j2\pi\left[ux_0(t)+vy_0(t)\right]}dt$$

Mathematical Modeling (5)

Suppose that the image undergoes uniform linear motion in the x-direction and y-direction, at a rate given by

$x_0(t) = at / T$ and $y_0(t) = bt / T$

$$H(u,v) = \int_0^T e^{-j2\pi[ux_0(t)+vy_0(t)]} dt$$

$$= \int_0^T e^{-j2\pi[ua+vb]t/T} dt$$

When the scene to be recorded translates relative to the camera at a constant velocity $v_{relative}$ under an angle of ϕ radians with the horizontal axis during the exposure interval $[0, t_{exposure}]$, the distortion is one-dimensional. Defining the "length of motion" by $L = v_{relative}\, t_{exposure}$, the PSF is given by:

$$d(x,y;L,\phi) = \begin{cases} \dfrac{1}{L} & \text{if } \sqrt{x^2+y^2} \le \dfrac{L}{2} \text{ and } \dfrac{x}{y} = -\tan\phi \\ 0 & \text{elsewhere} \end{cases} \tag{7a}$$

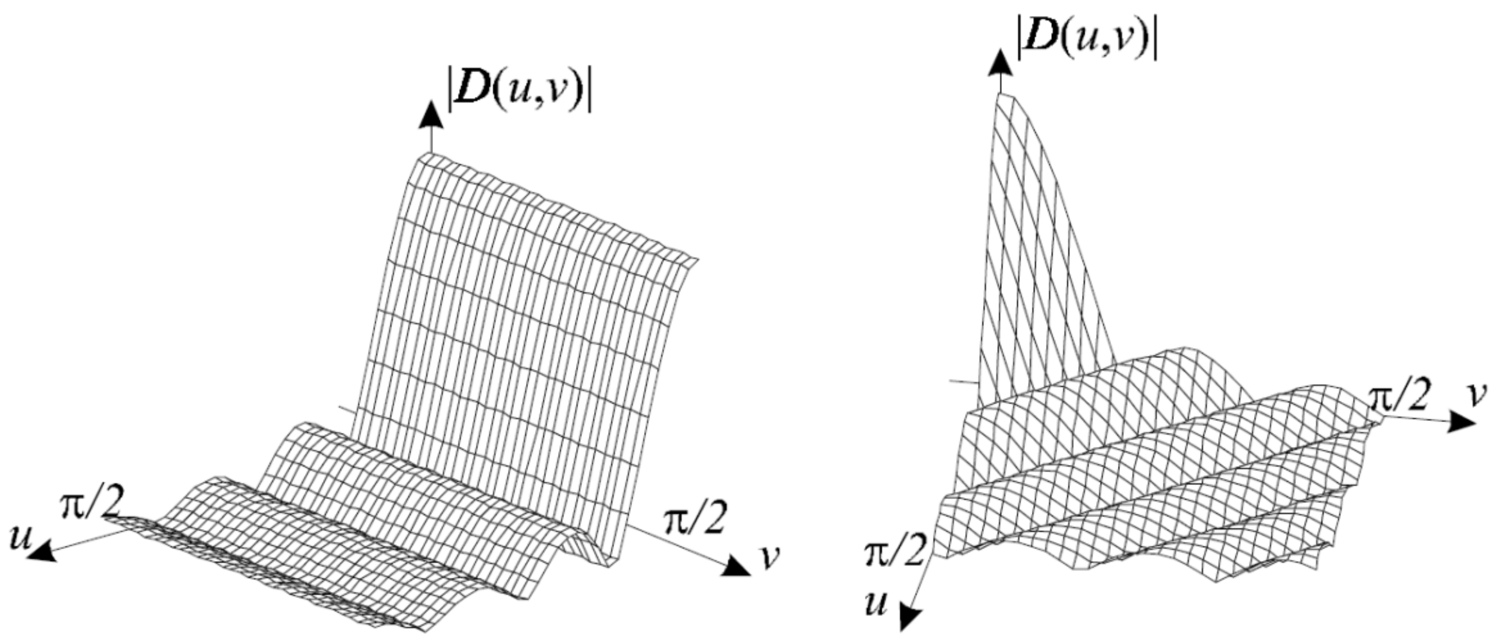

(a)

(b)

Figure 2: *PSF of motion blur in the Fourier domain, showing |D(u,v)|, for (a) L=7.5 and ϕ=0; (b) L=7.5 and ϕ=π/4*

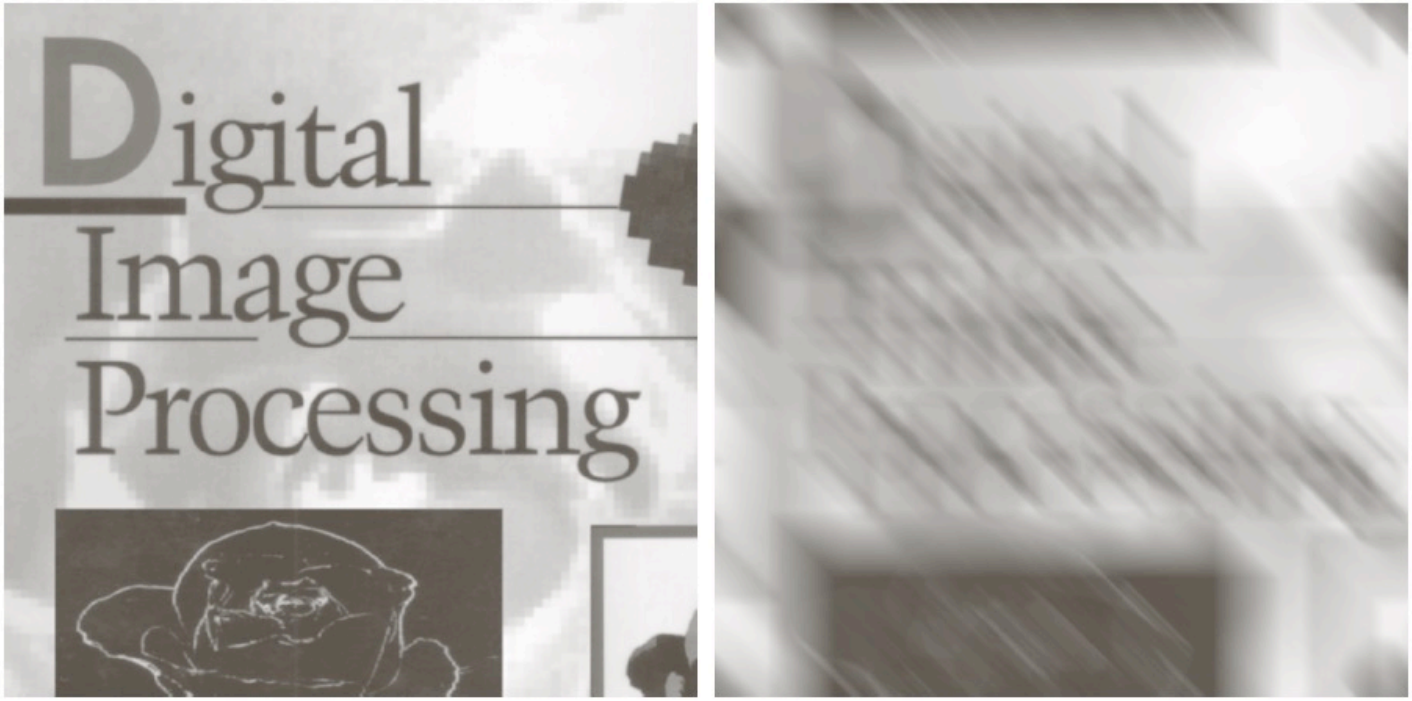

a b

FIGURE 5.26
(a) Original image.
(b) Result of blurring using the function in Eq. (5.6-11) with $a = b = 0.1$ and $T = 1$.

Inverse Filtering

An estimate of the transform of the original image

$$\hat{F}(u,v) = \frac{G(u,v)}{H(u,v)}$$

$$\hat{F}(u,v) = \frac{F(u,v)H(u,v) + N(u,v)}{H(u,v)}$$

$$= F(u,v) + \frac{N(u,v)}{H(u,v)}$$

Inverse Filtering

$$\hat{F}(u,v) = F(u,v) + \frac{N(u,v)}{H(u,v)}$$

1. We can't exactly recover the undegraded image because $N(u,v)$ is not known.

Inverse Filtering

EXAMPLE

The image in Fig. 5.25(b) was inverse filtered using the exact inverse of the degradation function that generated that image. That is, the degradation function is

$$H(u,v) = e^{-k\left[(u-M/2)^2+(v-N/2)^2\right]^{5/6}},\ k = 0.0025$$

Inverse Filtering

One approach is to limit the filter frequencies to values near the origin.

EXAMPLE

The image in Fig. 5.25(b) was inverse filtered using the exact inverse of the degradation function that generated that image. That is, the degradation function is

$$H(u,v) = e^{-k\left[\left(u-M/2\right)^2+(v-N/2)^2\right]^{5/6}}$$

$$k = 0.0025,\ M = N = 480.$$

a b
c d

FIGURE 5.27 Restoring Fig. 5.25(b) with Eq. (5.7-1). (a) Result of using the full filter. (b) Result with H cut off outside a radius of 40; (c) outside a radius of 70; and (d) outside a radius of 85.

A Butterworth lowpass function of order 10

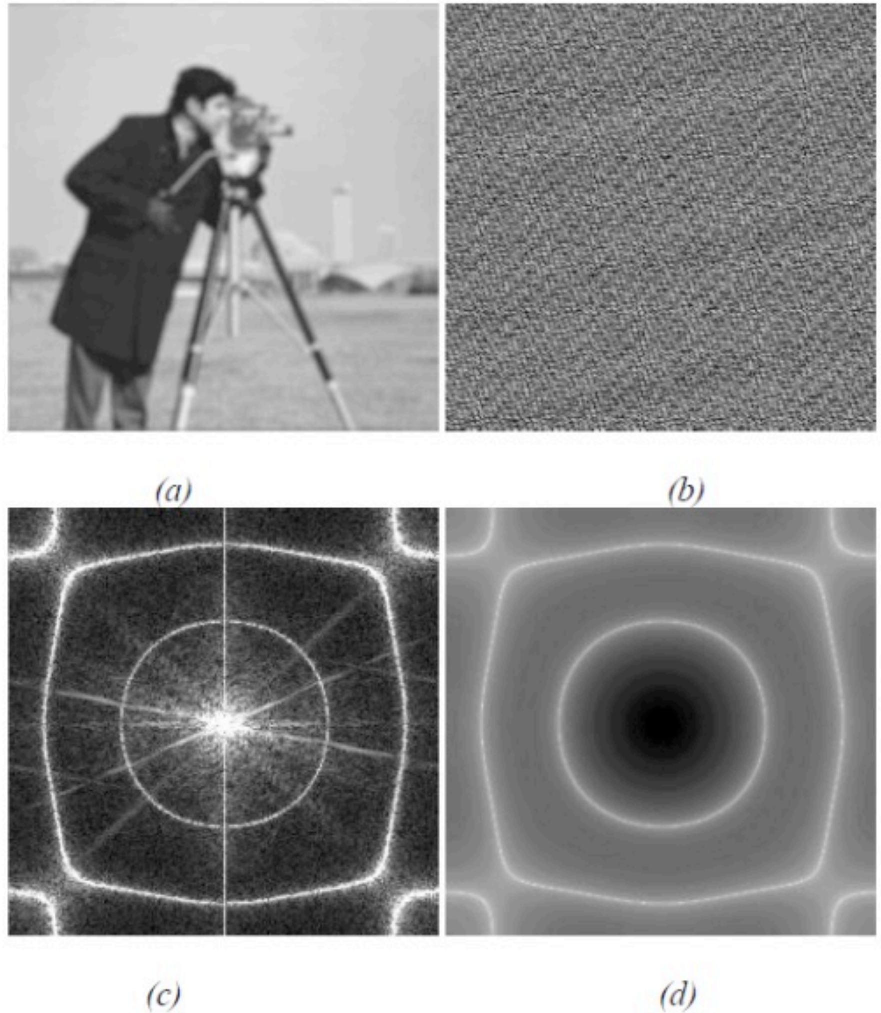

Figure 5: *(a) Image out-of-focus with SNR_g=10.3 dB (noise variance = 0.35) (b) Inverse filtered image, (c) Magnitude of the Fourier transform of the restored image. The DC component lies in the center of the image. The oriented white lines are spectral components of the image with large energy; (d) Magnitude of the Fourier transform of the inverse filter response.*

Minimum Mean Square Error (Wiener) Filtering

- **N. Wiener (1942)**

- **Objective**

  Find an estimate of the uncorrupted image such that the mean square error between them is minimized

$$e^2 = E\left\{(f - f)^2\right\}$$

Minimum Mean Square Error (Wiener) Filtering

The minimum of the error function is given in the frequency domain by the expression

$$F(u,v)=\left[\frac{H^*(u,v)S_f(u,v)}{S_f(u,v)\,|H(u,v)|^2+S_\eta(u,v)}\right]G(u,v)$$

$$=\left[\frac{H^*(u,v)}{|H(u,v)|^2+S_\eta(u,v)/S_f(u,v)}\right]G(u,v)$$

$$=\left[\frac{1}{H(u,v)}\frac{|H(u,v)|^2}{|H(u,v)|^2+S_\eta(u,v)/S_f(u,v)}\right]G(u,v)$$

Minimum Mean Square Error (Wiener) Filtering

$$F(u,v) = \left[\frac{1}{H(u,v)} \frac{|H(u,v)|^2}{|H(u,v)|^2 + S_\eta(u,v)/S_f(u,v)} \right] G(u,v)$$

$H(u,v)$: degradation function

$H^*(u,v)$: complex conjugate of $H(u,v)$

$|H(u,v)|^2 = H^*(u,v)H(u,v)$

$S_\eta(u,v) = |N(u,v)|^2 =$ power spectrum of the noise

$S_f(u,v) = |F(u,v)|^2 =$ power spectrum of the undegraded image

Minimum Mean Square Error (Wiener) Filtering

$$F(u,v)=\left[\frac{1}{H(u,v)}\frac{|H(u,v)|^2}{|H(u,v)|^2+K}\right]G(u,v)$$

K is a specified constant. Generally, the value of K is chosen interactively to yield the best visual results.

Minimum Mean Square Error (Wiener) Filtering

a b c

FIGURE 5.28 Comparison of inverse and Wiener filtering. (a) Result of full inverse filtering of Fig. 5.25(b). (b) Radially limited inverse filter result. (c) Wiener filter result.

Left: degradated image

Middle: inverse filtering

Right: Wiener filtering

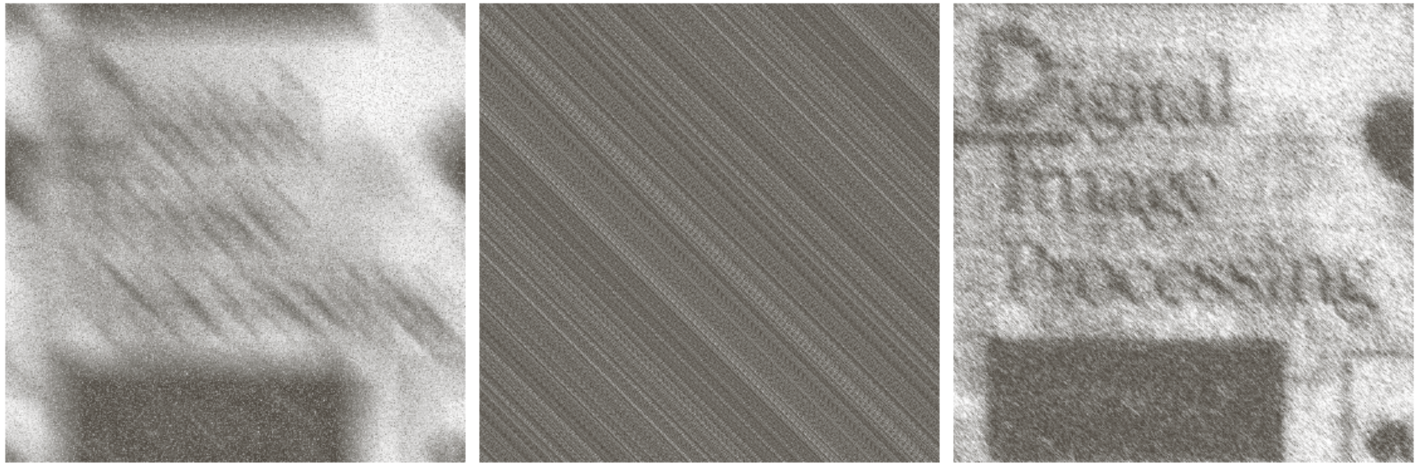

Some Measures (1)

Singal-to-Noise Ratio (SNR)

$$SNR = \frac{\sum_{u=0}^{M-1}\sum_{v=0}^{N-1} |F(u,v)|^2}{\sum_{u=0}^{M-1}\sum_{v=0}^{N-1} |N(u,v)|^2}$$

This ratio gives a measure of the level of information bearing singal power to the level of noise power.

Some Measures (2)

Mean Square Error (MSE)

$$\text{MSE}=\frac{1}{MN}\sum_{x=0}^{M-1}\sum_{y=0}^{N-1}\left[f(x,y)-f(x,y)\right]^2$$

Root-Mean-Sqaure-Error (RMSE)

$$\text{RMSE}=\frac{\sum_{u=0}^{M-1}\sum_{v=0}^{N-1} f(x,y)^2}{\sum_{u=0}^{M-1}\sum_{v=0}^{N-1}|f(x,y)-f(x,y)|^2}$$

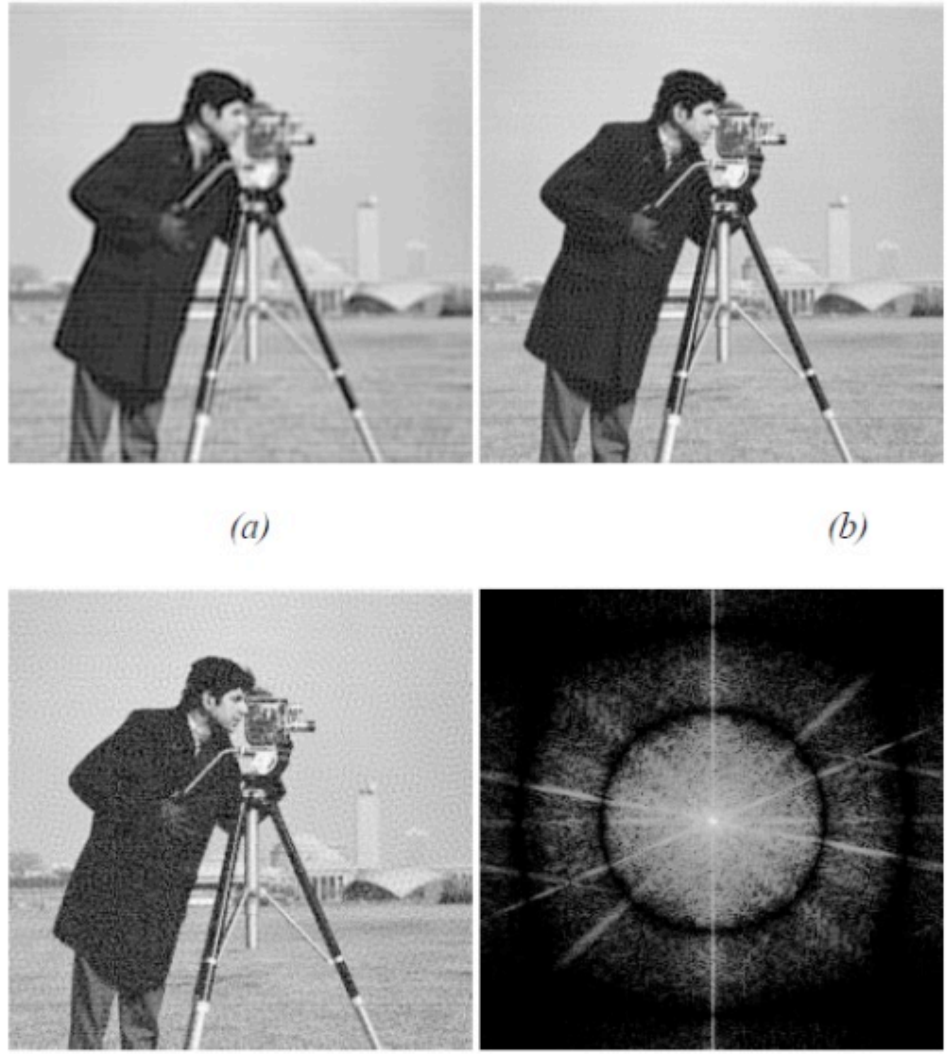

(a) (b)

(c) (d)

Figure 6: *(a) Wiener restoration of image in Figure 5(a) with assumed noise variance equal to 35.0 (ΔSNR=3.7 dB), (b) Restoration using the correct noise variance of 0.35 (ΔSNR=8.8 dB), (c) Restoration assuming the noise variance is 0.0035 (ΔSNR=1.1 dB). (d) Magnitude of the Fourier transform of the restored image in Figure 6b.*

Constrained Least Squares

spatially invariant linear filter. If the restoration is a good one, the blurred version of the restored image should be approximately equal to the recorded distorted image. That is:

$$h(n_1, n_2) * \hat{f}(n_1, n_2) \approx g(n_1, n_2) \qquad (21)$$

$$\hat{f} * h + \eta = g$$

With the inverse filter the approximation is made exact, which leads to problems because a match is made to noisy data. A more reasonable expectation for the restored image is that it satisfies:

$$\left\| g(n_1, n_2) - h(n_1, n_2) * \hat{f}(n_1, n_2) \right\|^2 = \sum_{k_1=0}^{N-1} \sum_{k_2=0}^{M-1} \left(g(k_1, k_2) - h(k_1, k_2) * \hat{f}(k_1, k_2) \right)^2 \approx \sigma_n^2 \qquad (22)$$

Constrained Least Squares Filtering

- In Wiener filter, the power spectra of the undegraded image and noise must be known. Although a constant estimate is sometimes useful, it is not always suitable.

- Constrained least squares filtering just requires the mean and variance of the noise.
- Minimize cost function C = sum over all pixels (x,y) in the image of $[\nabla^2 f(x,y)]^2$

  subject to:

$$\| g - H\hat{f} \|^2 = \| \eta \|^2$$

$$\hat{f} * h + \eta = g$$

Constrained Least Squares Filtering

$$F(u,v) = \left[\frac{H^*(u,v)}{|H(u,v)|^2 + \gamma |P(u,v)|^2} \right] G(u,v)$$

$P(u,v)$ is the Fourier transform of the function

$$p(x,y) = \begin{bmatrix} 0 & -1 & 0 \\ -1 & 4 & -1 \\ 0 & -1 & 0 \end{bmatrix}$$

γ is a parameter

Examples

a b c

FIGURE 5.30 Results of constrained least squares filtering. Compare (a), (b), and (c) with the Wiener filtering results in Figs. 5.29(c), (f), and (i), respectively.

Geometric Mean Filter

$$F(u,v)=\left[\frac{H^*(u,v)}{|H(u,v)|^2}\right]^{\alpha}\left[\frac{|H(u,v)|^2}{|H(u,v)|^2+\beta\left[S_\eta(u,v)/S_f(u,v)\right]}\right]^{1-\alpha}G(u,v)$$

$\alpha=1$: inverse filter

$\alpha=0$: parametric Wiener filter

$\alpha=1/2$: geometric mean filter

Image Reconstruction from Projection

- Reconstruct an image from a series of projections

  X-ray computed tomography (CT)

"Computed tomography is a medical imaging method employing tomography where digital geometry processing is used to generate a three-dimensional image of the internals of an object from a large series of two-dimensional X-ray images taken around a single axis of rotation."

http://en.wikipedia.org/wiki/Computed_tomography

Backprojection

“ In computed tomography or other imaging techniques requiring reconstruction from multiple projections, an algorithm for calculating the contribution of each voxel of the structure to the measured ray data, to generate an image; the oldest and simplest method of image reconstruction. “

http://www.medilexicon.com/medicaldictionary.php?t=9165

Image Reconstruction: Introduction

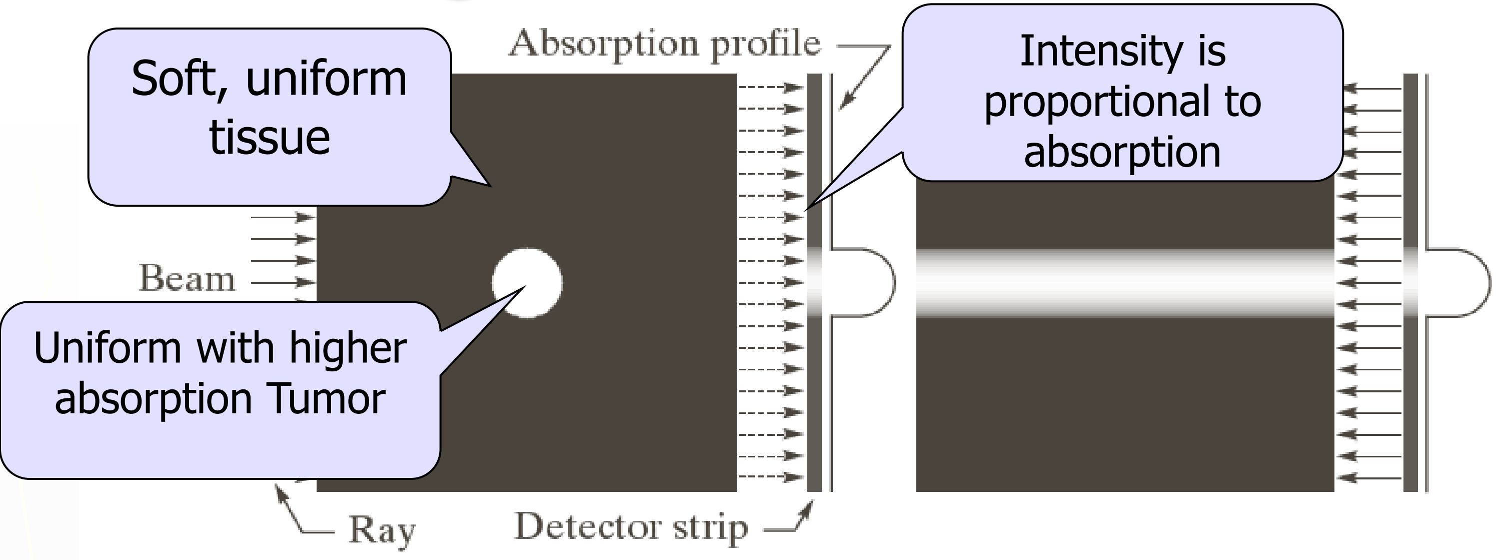

FIGURE 5.32
(a) Flat region showing a simple object, an input parallel beam, and a detector strip. (b) Result of back-projecting the sensed strip data (i.e., the 1-D absorption profile). (c) The beam and detectors rotated by 90°. (d) Back-projection. (e) The sum of (b) and (d). The intensity where the back-projections intersect is twice the intensity of the individual back-projections.

Image Reconstruction: Introduction

a	b	c
d	e	f

FIGURE 5.33 (a) Same as Fig. 5.32(a). (b)–(e) Reconstruction using 1, 2, 3, and 4 backprojections 45° apart. (f) Reconstruction with 32 backprojections 5.625° apart (note the blurring).

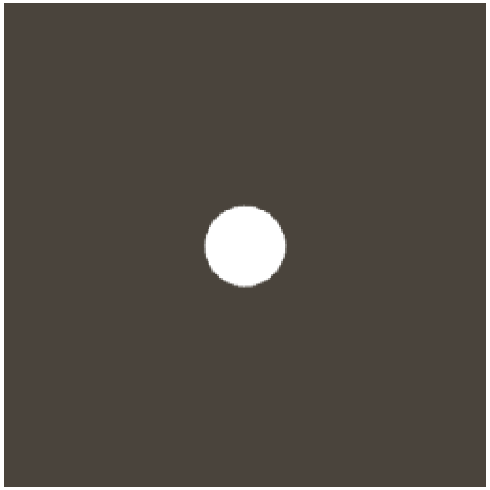

a	b	c
d	e	f

FIGURE 5.34 (a) A region with two objects. (b)–(d) Reconstruction using 1, 2, and 4 backprojections 45° apart. (e) Reconstruction with 32 backprojections 5.625° apart. (f) Reconstruction with 64 backprojections 2.8125° apart.

a	b
c	d

FIGURE 5.35 Four generations of CT scanners. The dotted arrow lines indicate incremental linear motion. The dotted arrow arcs indicate incremental rotation. The cross-mark on the subject's head indicates linear motion perpendicular to the plane of the paper. The double arrows in (a) and (b) indicate that the source/detector unit is translated and then brought back into its original position.

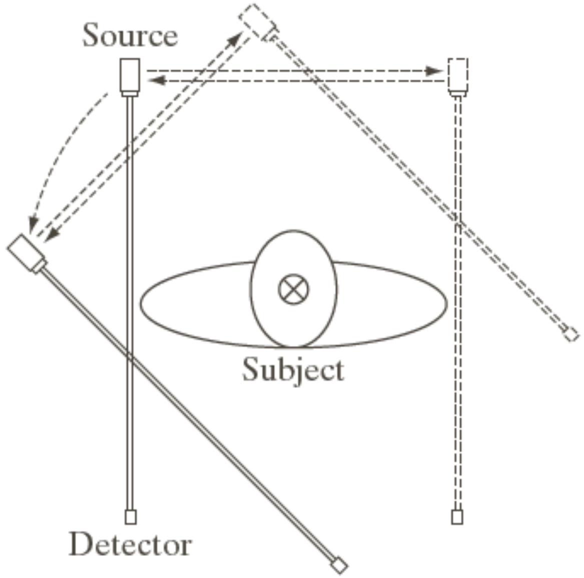

Other CTs

- **Electron beam CT** (Fifth-generation CT)

  Electron beam tomography (EBCT) was introduced in the early 1980s, by medical physicist Andrew Castagnini, as a method of improving the temporal resolution of CT scanners.

  High cost of EBCT equipment, and poor flexibility

- **Helical (or spiral) cone beam computed tomography** (sixth-generation)

  A type of three dimensional computed tomography (CT) in which the source (usually of x-rays) describes a helical trajectory relative to the object while a two dimensional array of detectors measures the transmitted radiation on part of a cone of rays emitting from the source

http://en.wikipedia.org/wiki/Computed_tomography

Other CTs

- Multislice CT (seventh-generation)

- The major benefit of multi-slice CT

  - Significant increase in detail
  - Utilizes X-ray tubes more economically
  - Reducing cost and potentially reducing dosage

Projections and the Radon Transform

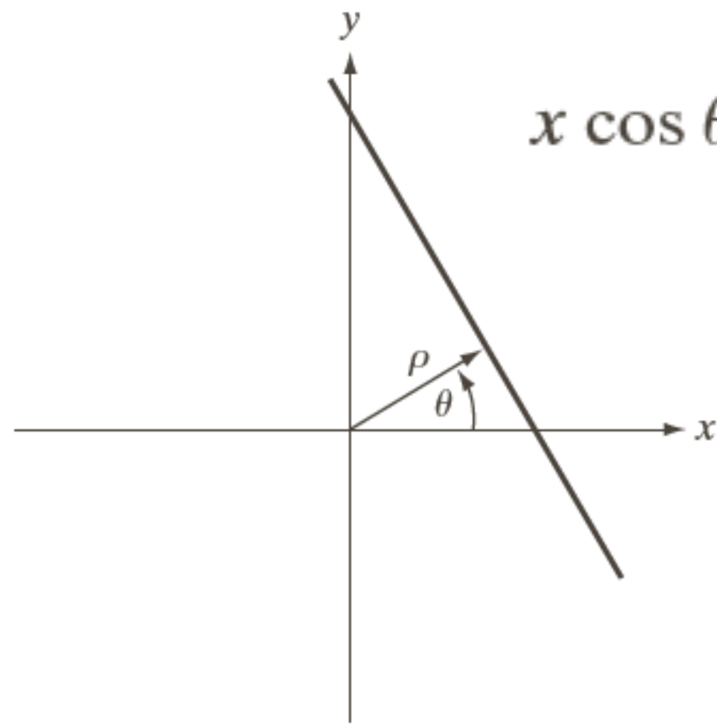

$$x \cos\theta + y \sin\theta = \rho$$

FIGURE 5.36 Normal representation of a straight line.

Projections and the Radon Transform

FIGURE 5.37 Geometry of a parallel-ray beam.

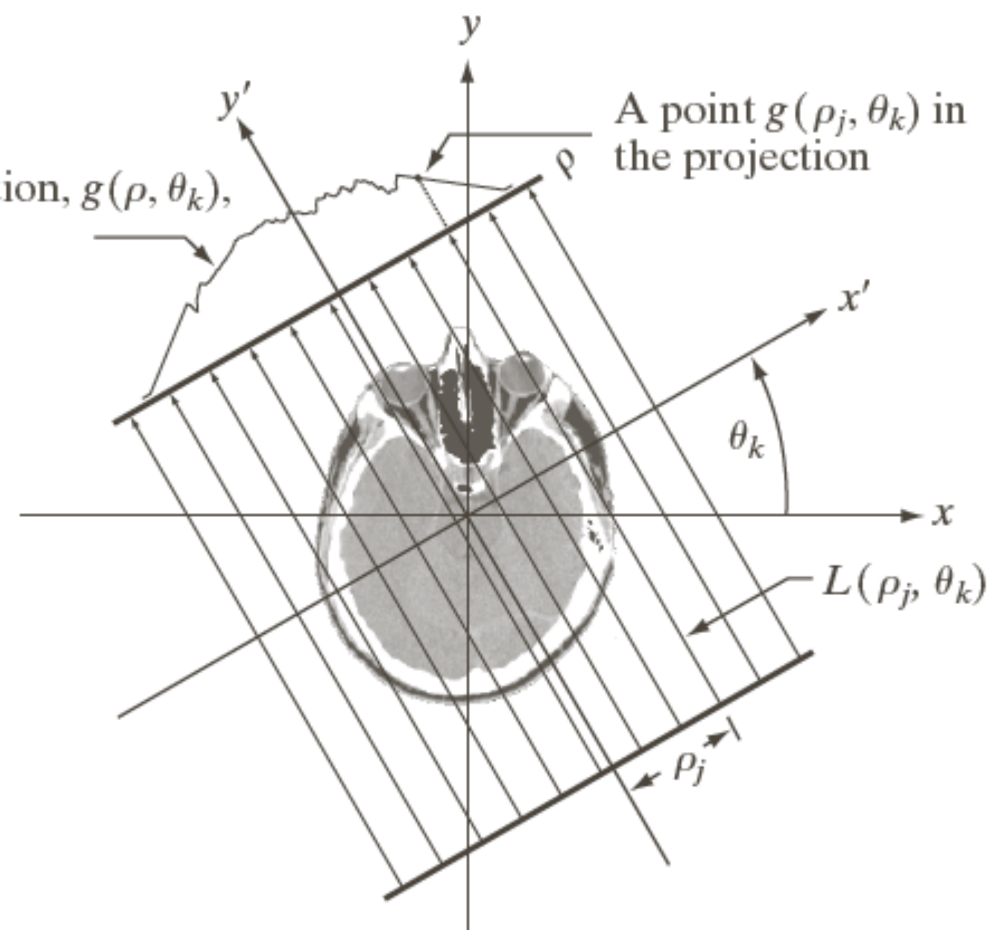

$$g(\rho_j, \theta_k) = \int_{-\infty}^{\infty}\int_{-\infty}^{\infty} f(x,y)\delta(x\cos\theta_k + y\sin\theta_k - \rho_j)dxdy$$

Projections and the Radon Transform

- **Radon transform** gives the projection (line integral) of f(x,y) along an arbitrary line in the xy-plane

$$\Re\{f\} = g(\rho,\theta) = \int_{-\infty}^{\infty}\int_{-\infty}^{\infty} f(x,y)\delta(x\cos\theta + y\sin\theta - \rho)dxdy$$

$$\Re\{f\} = g(\rho,\theta) = \sum_{x=0}^{M-1}\sum_{y=0}^{N-1} f(x,y)\delta(x\cos\theta + y\sin\theta - \rho)$$

Example: Using the Radon transform to obtain the projection of a circular region

- Assume that the circle is centered on the origin of the xy-plane. Because the object is circularly symmetric, its projections are the same for all angles, so we just check the projection for $\theta = 0$

$$f(x, y) = \begin{cases} A & x^2 + y^2 \le r^2 \\ 0 & \text{otherwise} \end{cases}$$

Example: Using the Radon transform to obtain the projection of a circular region

$$g(\rho,\theta)=\int_{-\infty}^{\infty}\int_{-\infty}^{\infty} f(x,y)\delta(x\cos\theta+y\sin\theta-\rho)dxdy$$

$$g(\rho) = \begin{cases} 2A\sqrt{r^2 - \rho^2} & |\rho| \le \mathrm{r} \\ 0 & \text{otherwise} \end{cases}$$

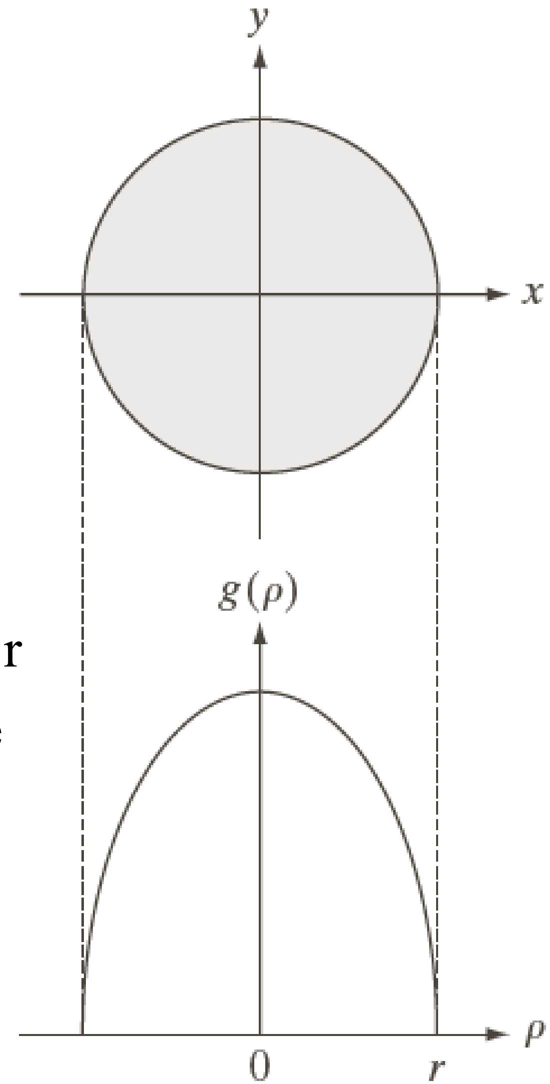

FIGURE 5.38 A disk and a plot of its Radon transform, derived analytically. Here we were able to plot the transform because it depends only on one variable. When g depends on both ρ and θ, the Radon transform becomes an image whose axes are ρ and θ, and the intensity of a pixel is proportional to the value of g at the location of that pixel.

Sinogram: The Result of Radon Transform

- Sinogram: the result of Radon transform is displayed as an image with ρ and θ as rectilinear coordinates

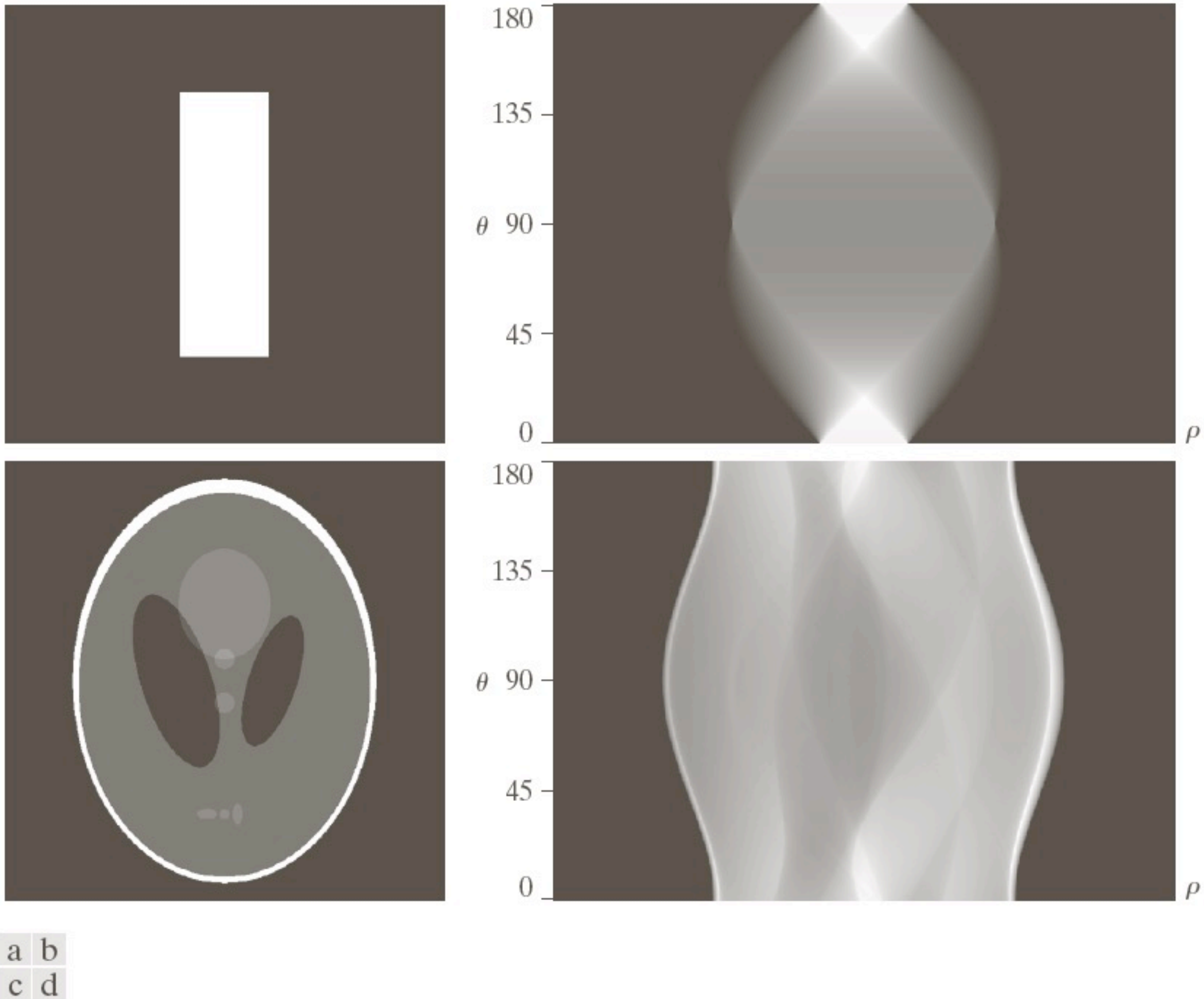

FIGURE 5.39 Two images and their sinograms (Radon transforms). Each row of a sinogram is a projection along the corresponding angle on the vertical axis. Image (c) is called the *Shepp-Logan phantom*. In its original form, the contrast of the phantom is quite low. It is shown enhanced here to facilitate viewing.

The Fourier-Slice Theorem

For a given value of θ, the 1-D Fourier transform of a projection with respect to ρ is

$$G(w,\theta) = \int_{-\infty}^{\infty} g(\rho,\theta) e^{-j2\pi\omega\rho} d\rho$$

$$G(\omega,\theta) = \int_{-\infty}^{\infty}\int_{-\infty}^{\infty}\int_{-\infty}^{\infty} f(x,y)\delta(x\cos\theta + y\sin\theta - \rho) e^{-j2\pi\omega\rho} d\rho dxdy$$

$$= \int_{-\infty}^{\infty}\int_{-\infty}^{\infty} f(x,y)\left[\int_{-\infty}^{\infty} \delta(x\cos\theta + y\sin\theta - \rho) e^{-j2\pi\omega\rho} d\rho\right] dxdy$$

$$= \int_{-\infty}^{\infty}\int_{-\infty}^{\infty} f(x,y) e^{-j2\pi\omega(x\cos\theta + y\sin\theta)} dxdy$$

The Fourier-Slice Theorem

$$G(w,\theta)=\int_{-\infty}^{\infty} g(\rho,\theta)e^{-j2\pi\omega\rho}d\rho$$

$$G(\omega,\theta)=\int_{-\infty}^{\infty}\int_{-\infty}^{\infty} f(x,y)e^{-j2\pi\omega(x\cos\theta+y\sin\theta)}dxdy$$

$$=\left[\int_{-\infty}^{\infty}\int_{-\infty}^{\infty} f(x,y)e^{-j2\pi(ux+vy)}dxdy\right]_{u=w\cos\theta,v=w\sin\theta}$$

$$=\left[F(u,v)\right]_{u=w\cos\theta,v=w\sin\theta}$$

$$=F(w\cos\theta,w\sin\theta)$$

Fourier-slice theorem: The Fourier tansform of a projection is a slice of the 2-D Fourier transform of the region from which the projection was obtained

Illustration of the Fourier-slice theorem

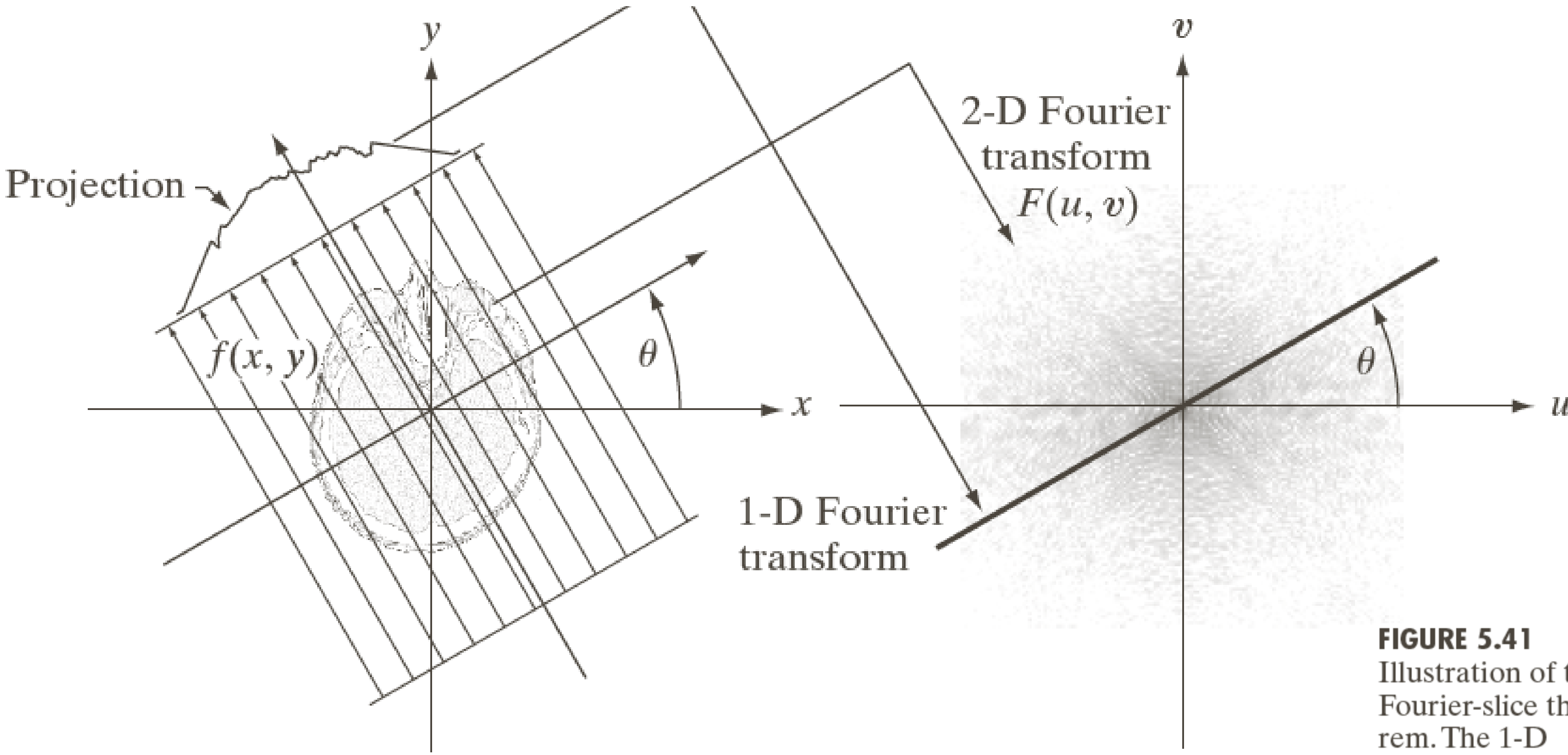

FIGURE 5.41 Illustration of the Fourier-slice theorem. The 1-D Fourier transform of a projection is a slice of the 2-D Fourier transform of the region from which the projection was obtained. Note the correspondence of the angle θ.

Reconstruction methods

1. Simple : - Nearest Neighbor (zero order interpolation)
   - First order interpolation.
2. Radon inversión formula
3. Iterative methods

Transform reconstruction

Polar Sampling: E.g.: 9 point DFT in each direction , 8 projections
The samples are equally spaced

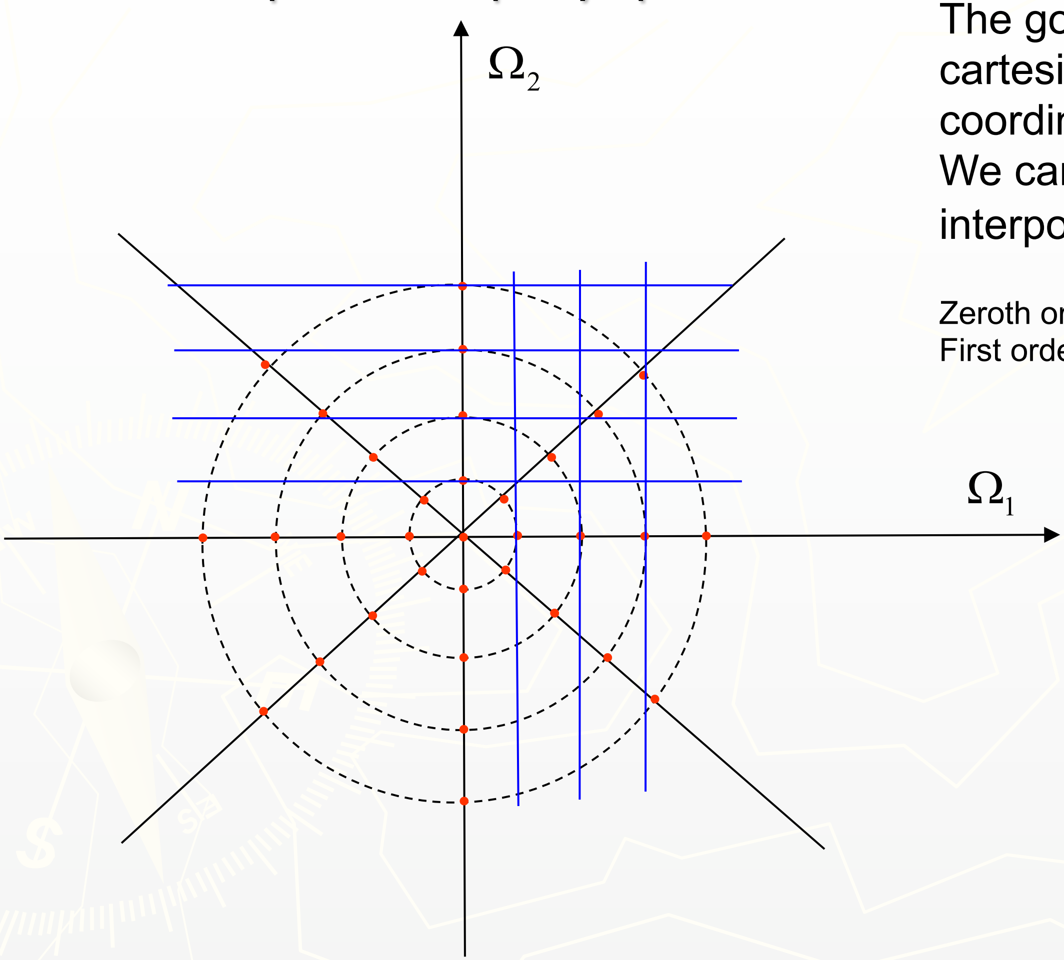

The goal is to find the FT values on the cartesian grid given the values at the polar coordinate system (red points)
We can then apply one of the following interpolation methods:

Zeroth order → Nearest Neighbor
First order → Weighed Sum of neighbor samples (Average)

Radon Inversion Formula

Recall that IDFT 2D of $Fc(\Omega_1, \Omega_2)$ is:

$$f_c(t_1,t_2)=\frac{1}{4\pi^2}\int_{\Omega_1=-\infty}^{+\infty}\int_{\Omega_2=-\infty}^{+\infty}F_c(\Omega_1,\Omega_2)\,e^{j\Omega_1 t_1}e^{j\Omega_2 t_2}\,d\Omega_1 d\Omega_2$$

We can express this expression using polar coordinates:

i.e.: $(\Omega_1, \Omega_2) \rightarrow (\omega, \theta)$.

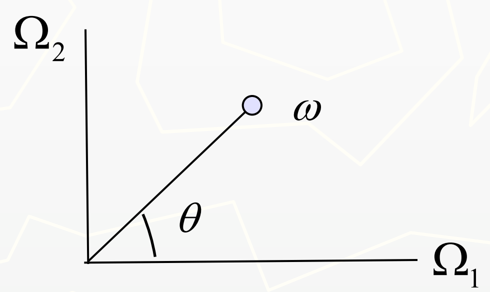

Radon Inversion Formula

To accomplish this we need the jacobian:

$$si \quad x = g(u,v) \quad y \quad y = h(u,v)\, i.e.:$$

$$\iint f(x,y)\,dxdy = \iint f(g(u,v),h(u,v))\,J\,dudv \quad where$$

$$J = \frac{\partial(x,y)}{\partial(u,v)} = \begin{vmatrix} \dfrac{\partial(x)}{\partial(u)} & \dfrac{\partial(x)}{\partial(v)} \\ \dfrac{\partial(y)}{\partial(u)} & \dfrac{\partial(y)}{\partial(v)} \end{vmatrix} = \frac{\partial(x)}{\partial(u)}\frac{\partial(y)}{\partial(v)} - \frac{\partial(y)}{\partial(u)}\frac{\partial(x)}{\partial(v)}$$

Radon Inversion Formula

$$si \quad \Omega_1 = g(\omega,\theta) = \omega\cos\theta \quad y \quad \Omega_2 = h(\omega,\theta) = \omega\, sen\,\theta$$

$$i.e.:$$

$$J = \frac{\partial(x,y)}{\partial(u,v)} = \begin{vmatrix} \cos\theta & -\omega sen\,\theta \\ sen\,\theta & \omega\cos\theta \end{vmatrix} = \omega$$

Therefore fc(t_1, t_2) will be:

$$f_c(t_1,t_2) = \frac{1}{4\pi^2}\int_0^{\pi}\int_{-\infty}^{+\infty} F_c(\omega\cos\theta, \omega\, sen\,\theta)\, e^{j\omega(t_1\cos\theta + t_2\, sen\,\theta)}\,|\omega|\; d\omega\, d\theta$$

Formula for inversion of Radon

Then we have:

$$f_c(t_1,t_2) = \frac{1}{4\pi^2}\int_0^{\pi}\int_{-\infty}^{+\infty} \underbrace{F_c(\omega\cos\theta, \omega\, sen\,\theta)}_{P_\theta(\omega)} e^{j\omega(t_1\cos\theta + t_2\, sen\,\theta)} \left|\omega\right| \; d\omega\, d\theta$$

$$f_c(t_1,t_2) = \frac{1}{4\pi^2}\int_0^{\pi}\underbrace{\int_{-\infty}^{+\infty} P_\theta(\omega)\, e^{j\omega(t_1\cos\theta + t_2\, sen\,\theta)} \left|\omega\right| \; d\omega}_{I}\, d\theta$$

Formula de inversion de Radon

The second integral is an IDFT:

$$f_c(t_1,t_2)=\frac{1}{4\pi^2}\int_0^{\pi}\underbrace{\int_{-\infty}^{+\infty} P_\theta(\omega)\,e^{j\omega(t_1\cos\theta+t_2\,sen\,\theta)}\left|\omega\right|\;d\omega\,d\theta}_{I}$$

IDFT

$$I=\int_{-\infty}^{+\infty} G_\theta(\omega)\,e^{j\omega t}\,d\omega \quad where:$$

$$G_\theta(\omega)=P_\theta(\omega)\left|\omega\right| \quad IDFT\left[G_\theta(\omega)\right]=g_\theta(t)$$

$$y\;\; t=t_1\cos\theta+t_2\,sen\,\theta$$

Formula de inversion de Radon

This gives us: $I = g_\theta(t)\Big|_{t=t_1\cos\theta + t_2\, sen\,\theta}$

$$I = g_\theta(t_1\cos\theta + t_2\, sen\,\theta)$$

Substituting in $fc(t_1, t_2)$ we have:

$$\boxed{f_c(t_1,t_2) = \frac{1}{4\pi^2}\int_0^\pi g_\theta(t_1\cos\theta + t_2\, sen\,\theta)\, d\theta}$$

Formula de inversion de Radon

Finally:

$$f_c(t_1,t_2) = \frac{1}{4\pi^2}\int_0^\pi g_\theta(t_1\cos\theta + t_2\,sen\,\theta)\,d\theta$$

$$G_\theta(\omega) = P_\theta(\omega)\left|\omega\right| \quad \Rightarrow g_\theta(t) = p(\theta,t) \otimes IDFT\left\{\left|\omega\right|\right\}$$

$$y \;\; t = t_1\cos\theta + t_2\,sen\,\theta$$

Radon Inversion Formula

Summary:

$$g_\theta(t) = p(\theta, t) \otimes IDFT\left\{|\omega|\right\} = \frac{d}{dt} \int_{-\infty}^{+\infty} \frac{P_\theta(\tau)}{t-\tau}\, d\tau$$

1- Find $p(\theta, t)$

2- Evaluate $g_\theta(t) = p(\theta, t) \otimes IDFT\left\{|\omega|\right\} = \frac{d}{dt} \int_{-\infty}^{+\infty} \frac{P_\theta(\tau)}{t-\tau}\, d\tau$

3- Substitute in fc(t_1, t_2)

$$f_c(t_1, t_2) = \frac{1}{4\pi^2} \int_0^\pi g_\theta(t_1 \cos\theta + t_2\, sen\, \theta)\, d\theta$$

Convolution Backprojection

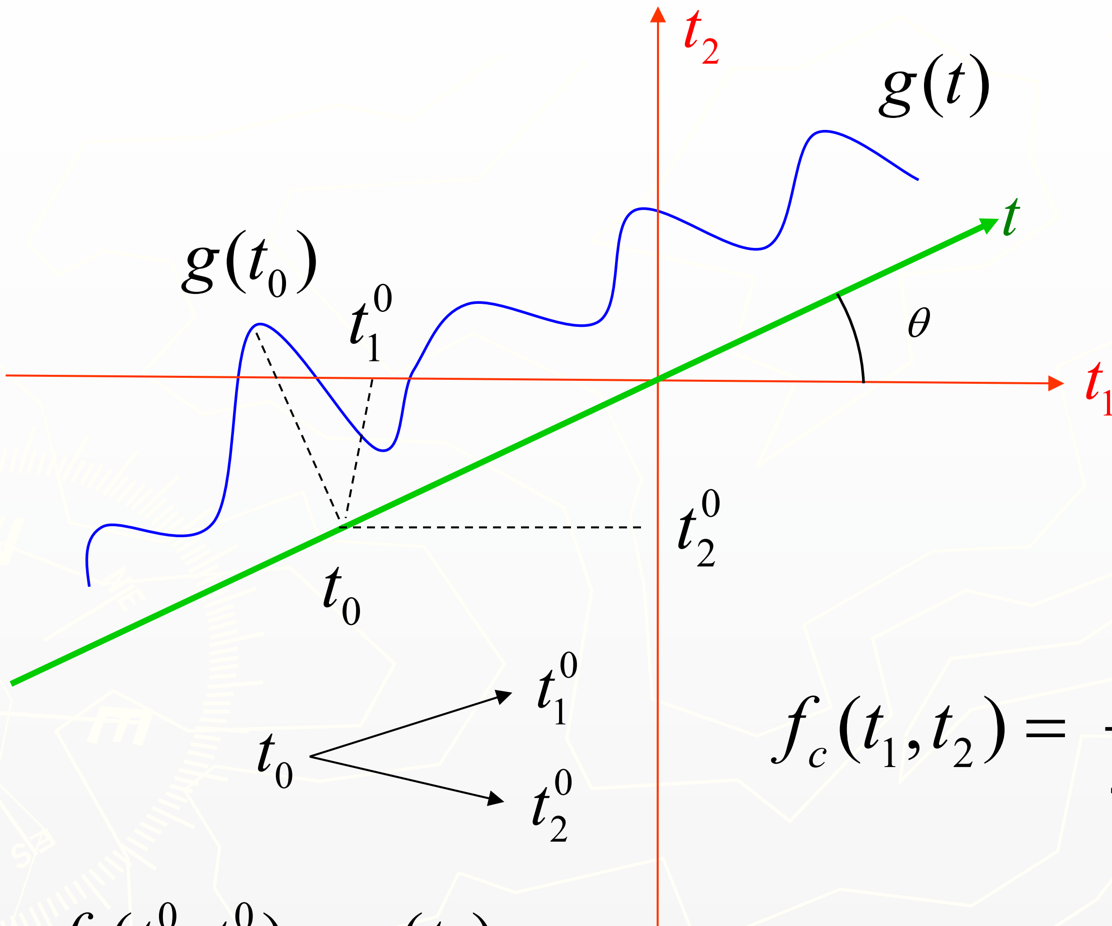

$$f_c(t_1, t_2) = \frac{1}{4\pi^2} \int_0^{\pi} g_\theta(t)\, d\theta$$

$$f_c(t_1^0, t_2^0) = g(t_0)$$

Reconstruction Using Parallel-Beam Filtered Backprojections

$$f(x,y)=\int_{-\infty}^{\infty}\int_{-\infty}^{\infty}F(u,v)e^{j2\pi(ux+vy)}dudv$$

Let $u=w\cos\theta, v=w\sin\theta$, then $dudv=wdwd\theta$,

$$f(x,y)=\int_{0}^{2\pi}\int_{0}^{\infty}F(w\cos\theta,w\sin\theta)e^{j2\pi w(x\cos\theta+y\sin\theta)}wdwd\theta$$

$$=\int_{0}^{2\pi}\int_{0}^{\infty}G(w,\theta)e^{j2\pi w(x\cos\theta+y\sin\theta)}wdwd\theta$$

$$G(w,\theta+180\ )=G(-w,\theta)$$

$$f(x,y)=\int_{0}^{\pi}\int_{-\infty}^{\infty}|w|G(w,\theta)e^{j2\pi w(x\cos\theta+y\sin\theta)}dwd\theta$$

Reconstruction Using Parallel-Beam Filtered Backprojections

$$f(x,y)=\int_0^{\pi}\int_{-\infty}^{\infty}|w|\,G(w,\theta)e^{j2\pi w(x\cos\theta+y\sin\theta)}dw\,d\theta$$

$$=\int_0^{\pi}\left[\int_{-\infty}^{\infty}|w|\,G(w,\theta)e^{j2\pi w\rho}dw\right]_{\rho=x\cos\theta+y\sin\theta}d\theta$$

It's not integrable

Approach:

Window the ramp so it becomes zero outside of a defined frequency interval. That is, a window band-limits the ramp filter.

Hamming / Hann Widow

$$h(w) = \begin{cases} c + (c-1)\cos\dfrac{2\pi w}{M-1} & 0 \le w \le (M-1) \\ 0 & \text{otherwise} \end{cases}$$

$c = 0.54$, the function is called the <u>Hamming window</u>

$c = 0.5$, the function is called the <u>Han window</u>

The Plot of Hamming Widow

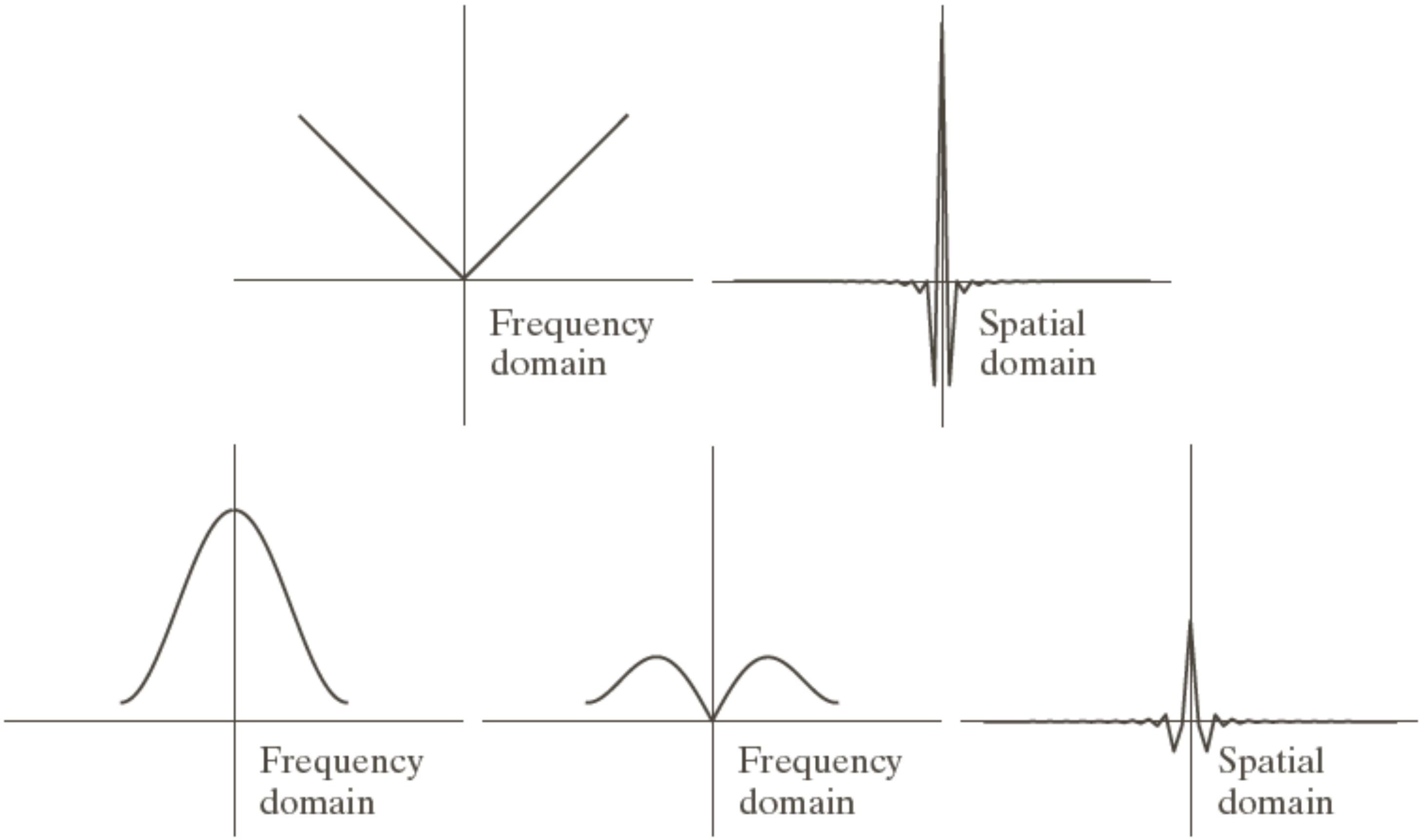

a b
c d e

FIGURE 5.42 (a) Frequency domain plot of the filter $|\omega|$ after band-limiting it with a box filter. (b) Spatial domain representation. (c) Hamming windowing function. (d) Windowed ramp filter, formed as the product of (a) and (c). (e) Spatial representation of the product (note the decrease in ringing).

Filtered Backprojection

The complete, filtered backprojection (to obtain the reconstructed image f(x,y)) is described as follows:

1. Compute the 1-D Fourier transform of each projection
2. Multiply each Fourier transform by the filter function |w| which has been multiplied by a suitable (e.g., Hamming) window
3. Obtain the inverse 1-D Fourier transform of each resulting filtered transform
4. Integrate (sum) all the 1-D inverse transforms from step 3

Examples: Filtered Backprojection

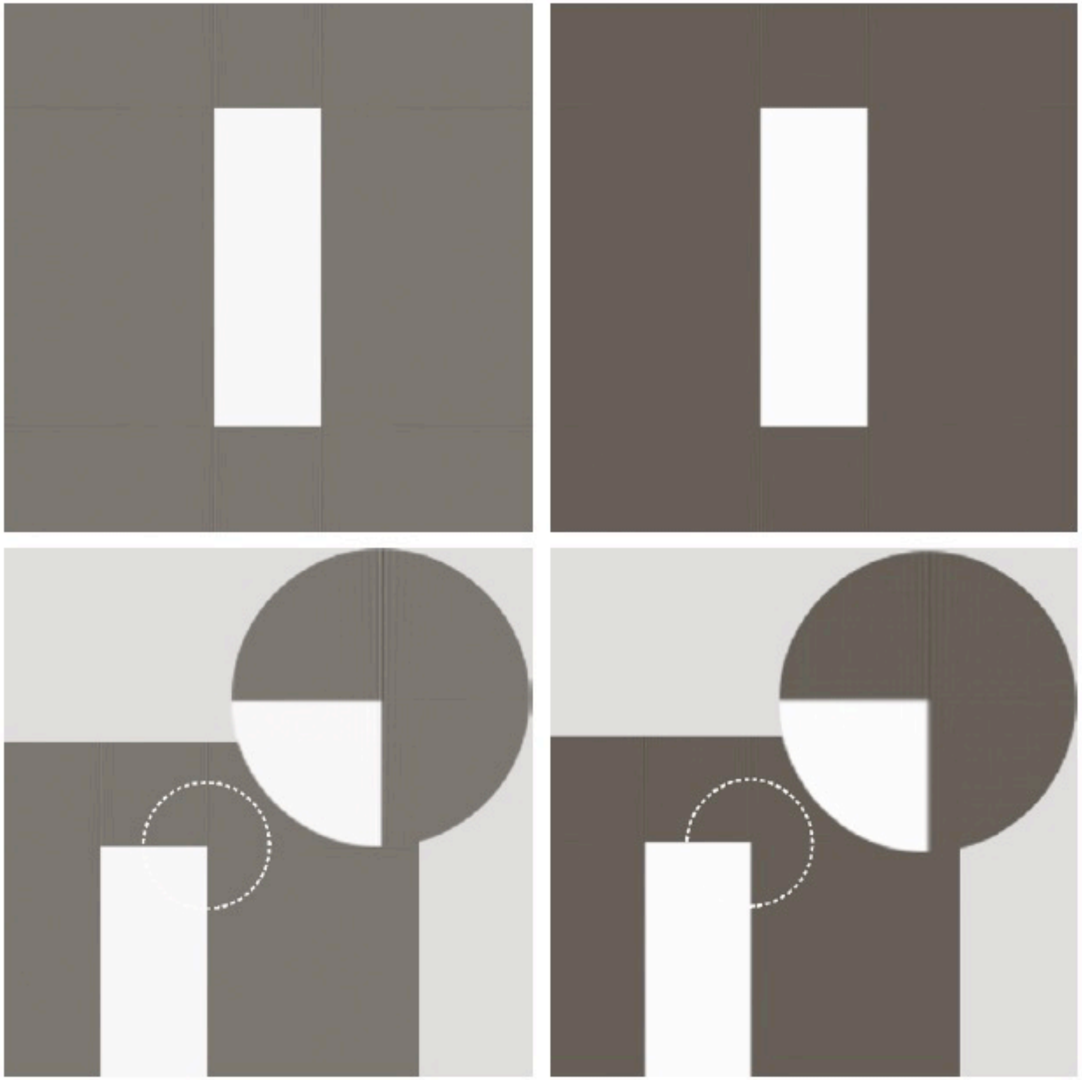

a	b
c	d

FIGURE 5.43 Filtered back-projections of the rectangle using (a) a ramp filter, and (b) a Hamming-windowed ramp filter. The second row shows zoomed details of the images in the first row. Compare with Fig. 5.40(a).

Examples: Filtered Backprojection

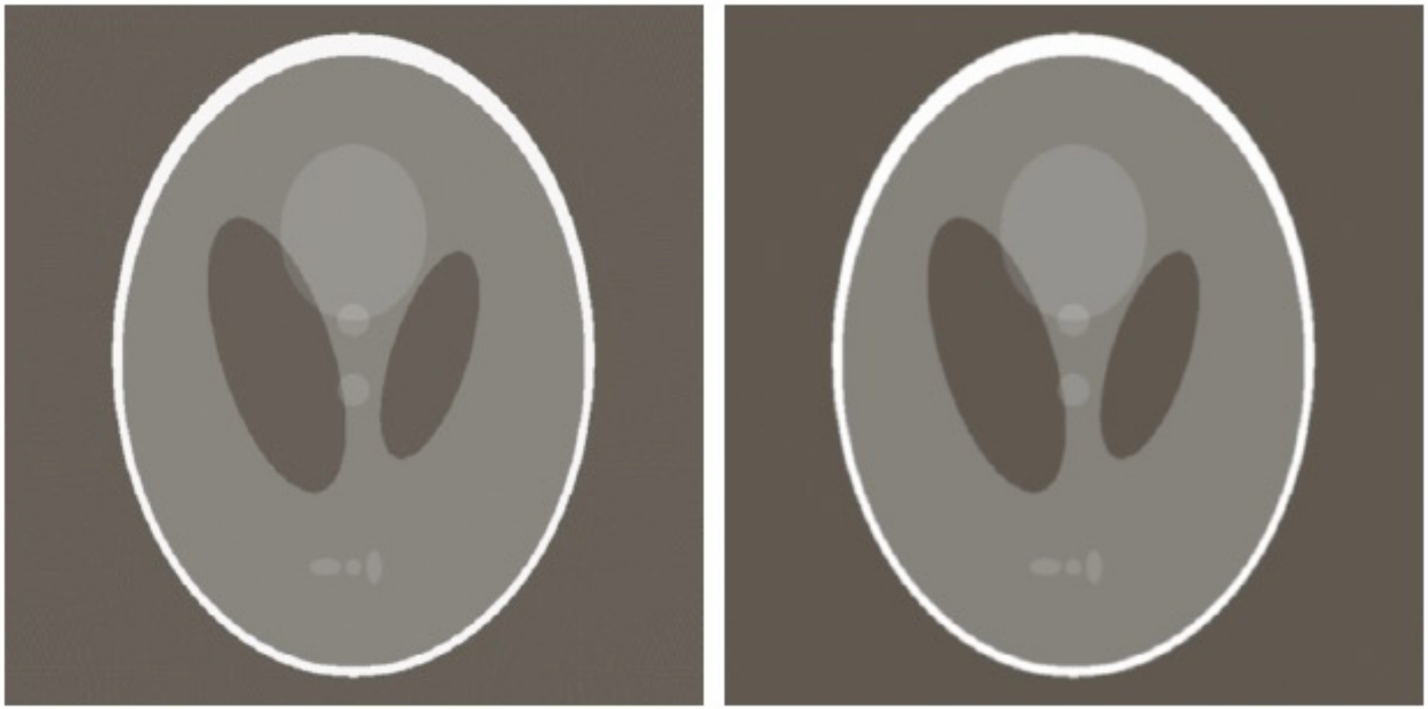

a b

FIGURE 5.44 Filtered backprojections of the head phantom using (a) a ramp filter, and (b) a Hamming-windowed ramp filter. Compare with Fig. 5.40(b).

Implementation of Filtered Backprojection in Spatial Domain

- Fourier transform of the product of two frequency domain functions is equal to the convolution of the spatial representation
- Let s(p) denote the inverse Fourier transform of |w|

$$f(x,y) = \int_0^{\pi} \left[\int_{-\infty}^{\infty} |w| G(w,\theta) e^{j2\pi w\rho} dw \right]_{\rho = x\cos\theta + y\sin\theta} d\theta$$

$$= \int_0^{\pi} \left[s(\rho) \bigstar g(\rho,\theta) \right]_{\rho = x\cos\theta + y\sin\theta} d\theta$$

$$= \int_0^{\pi} \left[\int_{-\infty}^{\infty} g(\rho,\theta) s(x\cos\theta + y\sin\theta - \rho) d\rho \right] d\theta$$